Steel 20MoCr4
Carburized Case (Vac 1700F)
Iteration #141 and 142

Monotonic Tensile
and Fatigue Test Results
Including Overload Tests

Prepared by:

Yikai Yin
and
Hong-Tae Kang

Department of Mechanical Engineering
College of Engineering and Computer Science
The University of Michigan-Dearborn
Dearborn, Michigan 48128

Prepared for:
The AISI Bar Steel Applications Group

September 2014

American Iron and Steel Institute
2000 Town Center, Suite 320
Southfield, Michigan 48075
tel: 248-945-4777
fax: 248-352-1740
www.autosteel.org

TABLE OF CONTENTS

NOMENCLATURE

A_o, A_f	initial, final area	S	engineering stress
HB, HRB, HRC	Brinell, Rockwell B-Scale, Rockwell C-Scale Hardness Number	YS, UYS, LYS, YS′	monotonic yield, upper yield, lower yield, cyclic yield strength
b, c, n	fatigue strength, fatigue ductility, strain hardening exponent	YPE	yield point elongation
D_o, D_f	initial, final diameter	S_u	ultimate tensile strength
e	engineering strain	EL%	percent elongation
E, E′	monotonic, cyclic strength coefficient	RA%	percent reduction in area
K, K′	monotonic, cyclic strength coefficient	σ, σ_f, σ_f'	true stress, true fracture strength, fatigue strength coefficient
L_o, L_f	initial, final gage length	ε_e, ε_p, ε	true elastic, plastic, total strain
$N_{50\%}$, $(N_f)_{10\%}$, $(N_f)_{50\%}$	number of cycles to midlife, 10% load drop, 50% load drop	ε_f, ε_f'	true fracture ductility, fatigue ductility coefficient
P_f, P_u	fracture, ultimate load	ε_a, ε_m, $\Delta\varepsilon$	strain amplitude, mean strain, strain range
R	strain ratio	$\Delta\varepsilon_e$, $\Delta\varepsilon_p$	elastic, plastic strain range

UNIT CONVERSION TABLE

Measure	SI Unit	US Unit	From SI to US	From US to SI
Length	mm	in	1 mm = 0.03937 in	1 in = 25.4 mm
Area	mm^2	in^2	1 mm^2 = 0.00155 in^2	1 in^2 = 645.16 mm^2
Load	kN	klb	1kN = 0.2248 klb	1 klb = 4.448 kN
Stress	MPa	ksi	1 MPa = 0.14503	1 ksi = 6.895 MPa
Temperature	^oC	^oF	^oC = (^oF - 32) /1.8	^oF = (^oC * 1.8) + 32

In SI Unit

1 kN = 10^3 N 1 Pa = 1 N/m^2 1 MPa = 10^6 Pa = 1 N/mm^2 1 GPa = 10^9 Pa

In US Unit

1 klb = 10^3 lb 1 psi = 1 lb/in^2 1 ksi = 10^3 psi

SUMMARY

Monotonic tensile properties and fatigue behavior data were obtained for steel material of iterations 141 and 142. The material was provided by AISI. Three tensile tests were performed to acquire the desired monotonic properties. Two tests gave similar results; the other one provided different result due to its bigger runout in center. Eleven constant amplitude strain-controlled fatigue tests at seven strain levels were performed to obtain the fatigue life and cyclic deformation curves and properties. The experimental procedure followed and results obtained are presented and discussed in this report. Periodic overload fatigue behavior and data were also obtained from six strain-controlled periodic overload fatigue tests. The experimental procedure followed and results obtained from periodic overload tests are also presented and discussed in this report. The experimental results showed that the lives of specimens with more than 0.006 inches runout in center are much shorter than those with less than 0.006 inches runout in center. In this study, we only analyze and discuss the fatigue behavior of the specimens with less than 0.006 inches runout in center.

I. EXPERIMENTAL PROGRAM

1.1 Material and Specimen Fabrication

1.1.1 Material

The steel material was provided by AISI. The test specimen was prepared from a 20MoCr4 steel grade with the condition of carburized case (Vac 1700F). The hardness of this material is 60 HRC (Courtesy of Chrysler). Inclusion distribution and microstructure of the material are shown in Figure 1 and 2, respectively.

1.1.2 Specimen

In this study, identical round specimens were used for monotonic and fatigue tests. The specimen configuration and dimensions are shown in Figure 3. This configuration deviates slightly from the specimens recommended by ASTM Standard E606 [1]. The recommended specimens have uniform gage sections. The specimen geometry shown in Figure 3 differs by using a large secondary radius in the gage section to compensate for the slight stress concentration at the gage to grip section transition.

All specimens were provided by AISI. Heat treatment and Machining were needed at first. The specimens were then polished prior to testing. Test specimens were protected immediately after machining and polishing until they were tested, since they may be susceptible to corrosion in moist room- temperature air. A report of the runout in center change before and after heat treatment for each AISI test bar is provided by AISI (See Table A.4). Before heat treatment, the runout in center of each specimen should not exceed 0.003 inches (0.076 mm). After the heat treatment, 0.006 inches (0.152 mm) will be the limit to determine whether we can get the acceptable experimental result for each specimen.

Before testing, the measurement of each specimen was needed. The measured dimensions are shown in Table A.3. Imprint specimen numbers on both ends of the test section in regions of low stress, away from grip contact surfaces.

1.2 Testing Equipment

1.2.1 Apparatus

A MTS 810 Material Test System which included a closed-loop sevro-controlled hydraulic axial load frame was used to conduct both monotonic and fatigue tests. The load cell used had a capacity of 100 kN. The MTS 646 Hydraulic Collet Grips with 0.50 in (12.7mm) diameter collets were employed to secure the specimens' ends in series with the load cell.

Total strain was controlled and measured using an extensometer rated as ASTM class B1 [2]. Here in this study, MTS Model 632.26E-20 Extensometer was chosen. The calibration of the extensometer was verified by the professional of the MTS. The extensometer had a gage length of 0.30 in and was capable of measuring strains up to 15%.

In order to protect the specimens' surface from the knife-edges of the extensometer, ASTM Standard E606 recommends the use of transparent tape or epoxy to 'cushion' the attachment. For this study, it was found that the application of transparent tape strips was difficult due to the size of the test section. Therefore, epoxy was considered to be the best protection. The tests were performed using M-coat A. Prior to the testing, made marks on both side of each specimen's gage length where the knife-edges of the extensometer can be set up. After each specimen was broken, observe the failure location and see if it is inside the gage length.

1.2.2 Alignment

Alignment of the load path components was essential for the accurate measurement of strain-life material constants. Significant effort was put forth to align the load path components (such as load cell, grips, specimens, and actuator). Misalignment can result from both tilt and offset between the central lines of the load train components. The alignment was done by the professional of the MTS in accordance with ASTM Standard E1012 [3].

1.3 Test Methods and Procedures

1.3.1 Monotonic tension tests

Monotonic tests in this study were performed using test methods specified by ASTM Standard E8 [4]. Two specimens were used to obtain the monotonic properties. One another specimen with big runout in center was used to compare the results with those two with small runout in center.

In order to protect the extensometer, strain control was used up to 10% strain, until the point of ultimate tensile strength had been crossed. After this point, displacement control was used until fracture. MTS 793.00 System Software and MTS 793.10 MultiPurpose Testware were used for the monotonic tests. The specimens are tested to fracture under strain or displacement control. For the elastic and initial yield region (0% to 0.5% strain) as well as the period up to which the extensometer was removed, a strain rate of 0.0025 in/in/min (0.001 mm/mm/s) was chosen. This strain rate was three-quarters of the maximum allowable rate specified by ASTM Standard E8 for the initial yield region. After the extensometer was removed, a displacement rate of 0.006 in/min (0.00254 mm/s) was used.

After the tension tests were concluded, the broken specimens were carefully reassembled. The final gage lengths of the fractured specimens, the final diameter, and the necking radius were then measured by a digital caliper for several times to make sure that the results were accurate. It should be noted that prior to the test, the initial diameter was measured with this same instrument.

1.3.2 Constant amplitude fatigue tests

Constant-amplitude axial fatigue tests provide information about the cyclic and fatigue behavior of materials. All constant amplitude fatigue tests in this study were performed according to ASTM Standard E606. It is recommended by this standard that at least 10 specimens by used to generate the fatigue properties. For this study, 11 specimens at 7 different strain amplitudes ranging from 0.20% to 0.50% were utilized. Among these specimens, five specimens were within the 0.006-inch limit runout in

center, the other six specimens were beyond the limit and then provided unacceptable results. Here in this study, we only analyze and discuss the fatigue behavior of the 5 acceptable specimens, whose runout in center were less than the 0.006-inch limit. MTS 793.00 System Software and MTS 793.10 MultiPurpose Testware were used in all strain-controlled tests. During each strain-controlled test, the total strain was recorded using the extensometer output. Test data were automatically recorded throughout each test.

There were two control modes used for these tests. Strain control was used in all tests with plastic deformation. For one of the elastic tests, strain control was used initially to determine the stabilized load, then load control was used for the reminder of the test and for the rest of the elastic tests, load control was used throughout. One reason for the change in control mode was due to the frequency limitation on the extensometer. Besides, at long lives, the total strain becomes quite small and the control of these quantities requires accurate instrumentation and extreme precision in the test procedure. Tests with anticipated lives exceeding 1 million cycles are change to load control mode when the load are stabilized. For the strain-controlled test, the applied frequencies ranged from 0.2 Hz to 5.0Hz in order to keep a strain rate about 0.02 in/in/sec. For the load-controlled tests, load waveforms with frequencies of up to 25Hz were used in order to shorten the overall test duration. All tests were conducted using a triangular waveform except the tests run at 25 Hz, when a sinusoidal waveform was used.

Failure of the specimens is defined when the maximum load decreases by 50% because of a crack or cracks being present. The strain-life curve is developed over a range of approximately 100 to 5,000,000 cycles (10,000,000 reversals).

1.3.3 Periodic overload fatigue tests

The overload tests were conducted to investigate the effects of periodic overloads on the fatigue life of smaller subsequent cycles. For this study, 6 specimens were tested at 5 different strain amplitudes. Among these specimens, 2 specimens were within the 0.006-inch limit runout in center, the other 4 specimens were beyond

the limit and then provided unacceptable results. Here in this study, we only analyze and discuss the fatigue behavior of the 2 acceptable specimens, whose runout in center were lower than the 0.006-inch limit. The periodic overload tests were run in strain-control with MTS 793.10 MultiPurpose Testware. During each strain-controlled test, the total strain was recorded using the extensometer output. Test data were automatically recorded throughout each test.

The input signal consisted of a periodic fully reversed overload of the type shown in Figure 11. The load history in these tests consisted of repeated load blocks made up of one fully-reversed overload cycle followed by a group of smaller constant amplitude cycles having the same maximum stress as the overload cycle. The overload cycles were applied at frequent intervals to maintain a low crack opening stress resulting in the subsequent cycles being fully open.

With this overload history, as the large cycles become more frequent, the fraction of the total damage done by them increases and that done by the small cycles decreases. The fully reversed strain amplitude for the overload cycle corresponded to 10^4 cycles to failure. The number of small cycles per block, N_{sc} were adjusted so that they cause 80 to 90% of the damage per block. Small cycle strain levels were selected at or below the run out level of the constant amplitude tests. Small cycles strain amplitudes were used from 0.175% to 0.100% and the number of small cycles per overload cycle ranged between 100 and 1000. For the specimens with less than 0.006 inches runout in center, the number of small cycles per overload cycle was chosen 500.

II. EXPERIMENTAL RESULTS AND ANALYSIS

2.1 Microstructural Data

A specimen was sectioned longitudinally from the grip end and transversely from the gage section to obtain a general microstructure description. The sample was prepared with standard test procedures for sectioning, mounting, polishing, and etched. The sample was reviewed and observed under a microscope. The microphotographs revealed the microstructure of the material. Figure 1 shows a low magnification photograph of the inclusion distribution in this kind of steel and Figure 2 shows a high magnification view of the microstructure from the gage area. Both of the figures were provided by Chrysler. The chemistry of the material is presented in Table 1.

2.2 Monotonic Deformation Behavior

The properties determined from monotonic tensile tests were the following: modulus of elasticity (E), yield strength (YS), ultimate tensile strength (S_u), percent elongation (%EL), percent reduction in area (%RA), true fracture strength (σ_f), true fracture ductility (ε_f), strength coefficient (K), and strain hardening exponent (n).

True stress (σ), true strain (ε), and true plastic strain (ε_p) were calculated from engineering stress (S) and engineering strain (e), according to the following relationships which are based on constant volume assumption:

$$\sigma = S(1 + e) \tag{1a}$$

$$\varepsilon = \ln(1 + e) \tag{1b}$$

$$\varepsilon_p = \varepsilon - \varepsilon_e = \varepsilon - \frac{\sigma}{E} \tag{1c}$$

The true stress (σ) - true strain (ε) plot is often represented by the Ramberg -Osgood equation:

$$\varepsilon = \varepsilon_e + \varepsilon_p = \frac{\sigma}{E} + \left(\frac{\sigma}{K}\right)^{\frac{1}{n}} \tag{2}$$

The strength coefficient, K, and strain hardening exponent, n, are the intercept and slope of the best line fit to true stress (σ) versus true plastic strain (ε_p) data in log-log scale:

$$\sigma = K\left(\varepsilon_p\right)^n \tag{3}$$

In accordance with ASTM Standard E739 [5], when performing the least squares fit, the true plastic strain (ε_p) was the independent variable and the true stress (σ) was the dependent variable. These plots for the two tests conducted are shown in Figure 4. As can be seen from this figure, the two curves are close to each other, their slope and intercept are similar with each other. To generate the K and n values, the range of data used in this figure was chosen according to the definition of discontinuous yielding specified in ASTM Standard E646 [6]. Therefore, the valid data range occurred between the end of yield point extension and the strain at maximum load.

The true fracture strength was corrected for necking according to the Bridgman correction factor [7]:

$$\sigma_f = \frac{\frac{P_f}{A_f}}{\left[1+\frac{4R}{D_f}\right]\ln\left[1+\frac{D_f}{4R}\right]} \tag{4}$$

where P_f is load at fracture, R is the neck radius, and D_f is the diameter at fracture.

The true fracture ductility, ε_f, was calculated from the relationship based on constant volume:

$$\varepsilon_f = \ln\left(\frac{A_0}{A_f}\right) = \ln\left(\frac{1}{1-RA}\right) \tag{5}$$

where A_f is the cross-sectional area at fracture, A_0 is the original cross-sectional area, and RA is the reduction in area.

A summary of the monotonic properties for this material is provided in Table A.1. The monotonic stress-strain curves are shown in Figure 5. As can be seen from this figure, the two curves are close to each other. Refer to Table A.1 for a summary of the monotonic test results.

To compare the tensile results between the big runout in center specimens and small runout in center specimens, Figure B.1 was provided at the Appendix B.

2.3 Cyclic Deformation Behavior

2.3.1 Transient cyclic response

Transient cyclic response describes the process of cyclic-induced change in deformation resistance of a material. Data obtained from constant amplitude strain-controlled fatigue tests were used to determine this response. Plots of stress amplitude variation versus applied number of cycles can indicate the degree of transient cyclic softening/hardening. Also, these plots show when cyclic stabilization occurs. A composite plot of the transient cyclic response for the steel studied is shown in Figure A.1a, while a semi-log plot is shown in Figure A.1b. Even though multiple tests were conducted at each strain amplitude, data from the small runout in center specimens at each strain amplitude tested are shown in these plots.

2.3.2 Steady-state cyclic deformation

Another cyclic behavior of interest was the steady state or stable response. Data obtained from constant amplitude strain-controlled fatigue tests were also used to determine this response. The properties determined from the steady-state hysteresis loops were the following: cyclic modulus of elasticity (E′), cyclic strength coefficient (K′), cyclic strain hardening exponent (n′), and cyclic yield strength (YS′). Half-life (midlife) hysteresis loops and data were used to obtain the stable cyclic properties.

Similar to monotonic behavior, the cyclic true stress-strain behavior can be characterized by Ramberg-Osgood type equation:

$$\frac{\Delta\varepsilon}{2} = \frac{\Delta\varepsilon_e}{2} + \frac{\Delta\varepsilon_p}{2} = \frac{\Delta\sigma}{2E} + \left(\frac{\Delta\sigma}{2K'}\right)^{\frac{1}{n'}} \quad (6)$$

It should be noted that in Equation 6 and the other equations that follow, E is the average modulus of elasticity that was calculated from the monotonic tests.

The cyclic strength coefficient, K′, and cyclic strain hardening exponent, n′, are the intercept and slope of the best line fit to true stress amplitude ($\Delta\sigma/2$) versus true plastic strain amplitude ($\Delta\varepsilon_p/2$) data in log-log scale:

$$\frac{\Delta\sigma}{2} = K'\left(\frac{\Delta\varepsilon_p}{2}\right)^{n'} \quad (7)$$

In accordance with ASTM Standard E739 [5], when performing the least squares fit, the true plastic strain amplitude ($\Delta\varepsilon_p/2$) was the independent variable and the stress amplitude ($\Delta\sigma/2$) was the dependent variable. The true plastic strain amplitude was calculated by the following equation:

$$\frac{\Delta\varepsilon_p}{2} = \frac{\Delta\varepsilon}{2} - \frac{\Delta\sigma}{2E} \quad (8)$$

To generate the K′ and n′ values, the range of data used in this figure was chosen for $\left[\frac{\Delta\varepsilon_p}{2}\right]_{calculated} \geq 0.001$ in/in. This relationship could not be plotted in this study, since the specimens only undergone the elastic range, there is nearly no plastic deformation, and then no plastic properties could be generated.

The cyclic stress-strain curve reflects the resistance of a material to cyclic deformation and can be vastly different from the monotonic stress-strain curve. The cyclic stress-strain curve is shown in Figure 6. In Figure 7, superimposed plots of monotonic and cyclic curves are shown. As can be seen in this figure, the material cyclically hardened. Figure A.2 shows a composite plot of the steady-state (midlife) hysteresis loops. Even though multiple tests were conducted at each strain amplitude, the stable loops from only the small runout in center specimens test at each strain amplitude are shown in this plot.

2.4 Constant Amplitude Fatigue Behavior

Constant amplitude strain-controlled fatigue tests were performed to determine the strain-life curve. The following equation relates the true strain amplitude to the fatigue life:

$$\frac{\Delta\varepsilon}{2} = \frac{\Delta\varepsilon_e}{2} + \frac{\Delta\varepsilon_p}{2} = \frac{\sigma_f'}{E}\left(2N_f\right)^b + \varepsilon_f'\left(2N_f\right)^c \quad (9)$$

where σ_f' is the fatigue strength coefficient, b is the fatigue strength exponent, ε_f' is the fatigue ductility coefficient, c is the fatigue ductility exponent, E is the monotonic modulus of elasticity, and $2N_f$ is the number of reversals to failure.

The fatigue strength coefficient, σ_f', and fatigue strength exponent, b, are the intercept and slope of the best line fit to true stress amplitude ($\Delta\sigma/2$) versus reversals to failure ($2N_f$) data in log-log scale:

$$\frac{\Delta\sigma}{2} = \sigma_f'\left(2N_f\right)^b \tag{10}$$

In accordance with ASTM Standard E739 [5], when performing the least squares fit, the stress amplitude ($\Delta\sigma/2$) was the independent variable and the reversals to failure ($2N_f$) was the dependent variable. This plot is shown in Figure 8. To generate the σ_f' and b values, all data, with the exception of the run-out tests, in the stress-life figure were used. To compare the stress-life results between the big runout in center specimens and small runout in center specimens, Figure B.2 was provided at the Appendix B.

The fatigue ductility coefficient, ε_f', and fatigue ductility exponent, c, are the intercept and slope of the best line fit to calculated true plastic strain amplitude ($\Delta\varepsilon_p/2$) versus reversals to failure ($2N_f$) data in log-log scale:

$$\left(\frac{\Delta\varepsilon_p}{2}\right)_{calculated} = \varepsilon_f'\left(2N_f\right)^c \tag{11}$$

In accordance with ASTM Standard E739 [5], when performing the least squares fit, the true plastic strain amplitude ($\Delta\varepsilon_p/2$) was the independent variable and the reversals to failure ($2N_f$) was the dependent variable. The calculated true plastic strain amplitude was determined from Equation 8. To generate the ε_f' and c values, the range of data used in this figure was chosen for $\left[\frac{\Delta\varepsilon_p}{2}\right]_{calculated} \geq 0.001$ in/in. This relationship could not be plotted in this study, since the specimens only undergone the elastic range, there is nearly no plastic deformation, and then no plastic properties could be generated.

The true strain amplitude versus reversals to failure plot is shown in Figure 9. This plot displays the strain-life curve (Eqn. 9), the elastic strain portion (Eqn. 10), the plastic strain portion (Eqn. 11) and superimposed fatigue data. A summary of the cyclic properties for this steel is provided in Table 2. Table A.2 provides the summary of the fatigue test results.

To compare the strain-life results between the big runout in center specimens and

small runout in center specimens, Figure B.3 was provided at the Appendix B.

A parameter often used to characterize fatigue behavior at stress concentrations, such as at the root of a notch, is Neuber parameter [7]. Neuber's stress range is given by:

$$\sqrt{(\Delta\varepsilon)(\Delta\sigma)E} = 2\sqrt{\left(\sigma_f'\right)^2\left(2N_f\right)^{2b} + \sigma_f'\varepsilon_f'E\left(2N_f\right)^{b+c}} \tag{12}$$

A plot of Neuber stress range versus reversals to failure is shown in Figure 10. This figure displays the Neuber curve based on Eqn. 12 and superimposed fatigue data for this material.

2.5 Periodic Overload Fatigue Behavior

Periodic Overload strain-controlled fatigue tests were performed to determine the effective strain-life curve. The effective strain-life curve is plotted using the strain amplitude of the small cycles in the overload block and the calculated equivalent life. The equivalent fatigue lives for the smaller cycles were obtained using the linear damage rule:

$$\frac{N_{OL}}{N_{f,OL}} + \frac{N_{SC}}{N_{f,SC(eq)}} = 1 \tag{13}$$

Where N_{OL} is the number of overload cycles in a periodic overload test, $N_{f,OL}$ is the number of cycles to failure if only overloads were applied in a test, N_{SC} is the number of smaller cycles in a periodic overload test, and $N_{f,SC(eq)}$ is the computed equivalent fatigue life for the smaller cycles.

The linear damage rule was also used to calculate the cumulative damage of the overload cycles, D_{OL}, as

$$\frac{N_{OL}}{N_{f,OL}} = D_{OL} \tag{14}$$

Figure 12 shows the effective strain-life data superimposed on the constant amplitude strain life plot. Table A.5 presents a summary of the periodic overload test results. To compare the overload results between the big runout in center specimens

and small runout in center specimens, Figure B.4 was provided at the Appendix B.

A plot of the SWT parameter for both the constant amplitude and overload data provides another method of comparison between the two sets of data, where the mean stress present in the small cycles is taken into account. The SWT parameter is given by

$$\sigma_{max}\varepsilon_a = \frac{1}{E}\left[\left(\sigma_f'\right)^2\left(2N_f\right)^{2b} + \sigma_f'\varepsilon_f' E\left(2N_f\right)^{b+c}\right] \quad (15)$$

where $\sigma_{max} = \sigma_m + \sigma_a$. The SWT plot is shown in Figure 13. As in the constant amplitude strain-life curve, the overload data and effective strain-life curve diverged from the constant amplitude curve.

Plots of the overload cycle and small cycle stress amplitude variation versus applied number of blocks can indicate the degree of transient cyclic soften/hardening. Also, these plots show when cyclic stabilization occurs over the life of the specimen. A composite plot of the small cycle transient cyclic response for the steel studied is shown in Figure A.3. A composite plot of the overload cycle transient cyclic response is shown in Figure A.4. The amplitude of the transient response is shown in the Figure A.3a and A.4a while the mean of the transient response is shown in Figure A.3b and A.4b. Data from the small (less than 0.006 inches) runout in center specimens at each strain amplitude tested are shown in these plots. Stress response of small cycles was also evaluated within a single block. This can be seen in Figure A.5b, which is a plot of the mean stress at each strain level within a single block at midlife and in Figure A.5a, which shows the stress amplitude at each strain level within a single block at midlife. In this study, the #200 block was chosen at each strain amplitude to get the stress values, data from each test are shown in these plots. These plots show steady state stress response within a load block.

The midlife hysteresis loops for each small cycle strain level are shown in Figures A.6a and A.6b. The small cycle loop was taken from the mid-cycle of the midlife block.

Table 1: Chemical Composition of Steel 8615 (Courtesy of Chrysler)

Element	Wt.%
Carbon, C	0.210%
Manganese, Mn	0.750%
Phosphorus, P	0.011%
Sulfur, S	0.026%
Silicon, Si	0.300%
Nickel, Ni	0.009%
Chromium, Cr	0.480%
Molybdenum, Mo	0.440%
Copper, Cu	0.190%
Tin, Sn	0.008%
Aluminum, Al	0.028%
Vanadium, V	0.005%
Calcium, Ca	0.0008%
Niobium, Nb	0.002%
Nitrogen , N	0.0098%

Table 2: Summary of the Mechanical Properties

Monotonic Properties	Average	Range
Modulus of elasticity, E, GPa:	202.7	201.1 - 204.3
Yield strength (0.2% offset), YS, MPa:	-	-
Ultimate strength, S_u, MPa:	964.8	952.4 – 977.1
Percent elongation, %EL (%):	3.28%	3.00% - 3.57%
Percent reduction in area, %RA (%):	0%	0% - 0%
Strength coefficient, K, MPa:	3998.1	3660.1 – 4336.1
Strain hardening exponent, n:	0.2116	0.1967 - 0.2264
True fracture strength, σ_f, MPa:	685.2	676.7 – 693.7
True fracture ductility, ε_f (%):	0%	0% - 0%
Hardness, HRC	60	

Cyclic Properties	Average	Range
Cyclic modulus of elasticity, E', GPa:	202.2	198.3 – 205.9
Fatigue strength coefficient, σ_f', MPa:	2015.3	
Fatigue strength exponent, b:	-0.101	
Fatigue ductility coefficient, ε_f':	-	
Fatigue ductility exponent, c:	-	
Cyclic strength coefficient, K', MPa:	-	
Cyclic strain hardening exponent, n':	-	
Cyclic yield strength, YS', MPa:	-	
Fatigue Limit (defined at 10^6 cycles), MPa	499.3	

Figure 1: Low magnification photograph of the inclusion distribution in the steel (Courtesy of Chrysler)

Figure 2: High magnification photo showing the microstructure of the transverse section from the gage area (Courtesy of Chrysler)

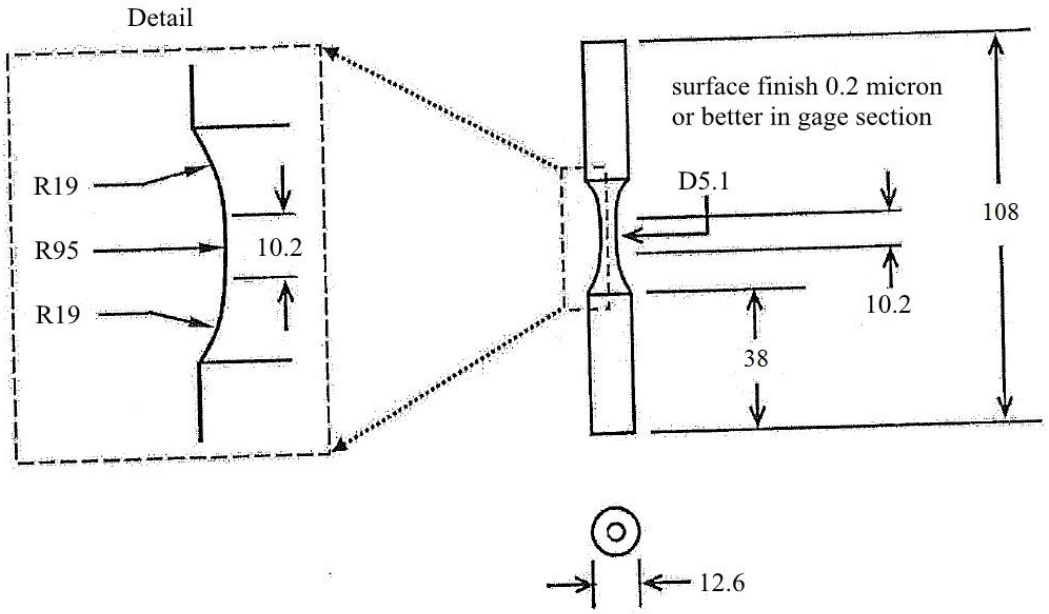

Figure 3: Specimen configuration and dimensions (mm)

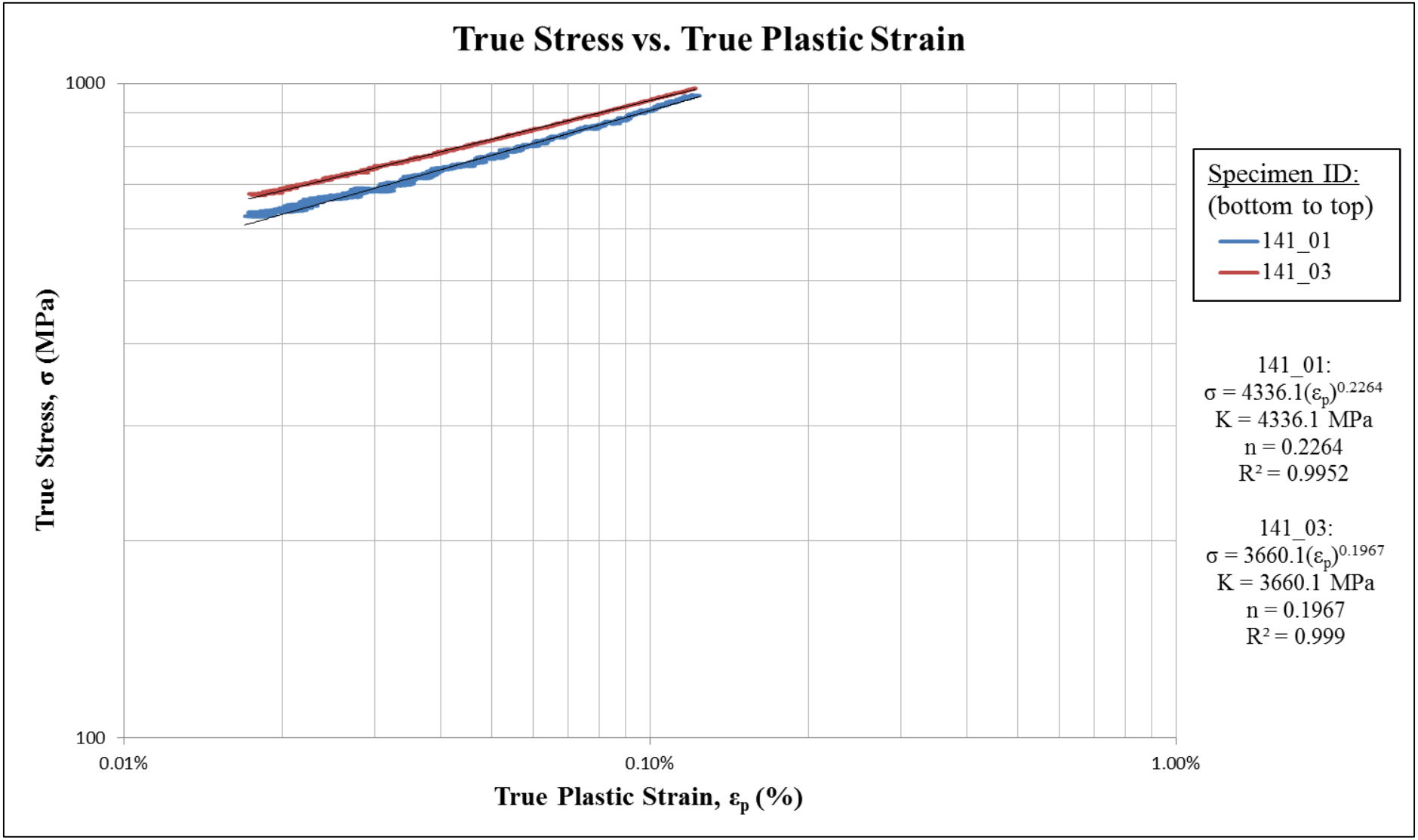

Figure 4: True stress versus true plastic strain

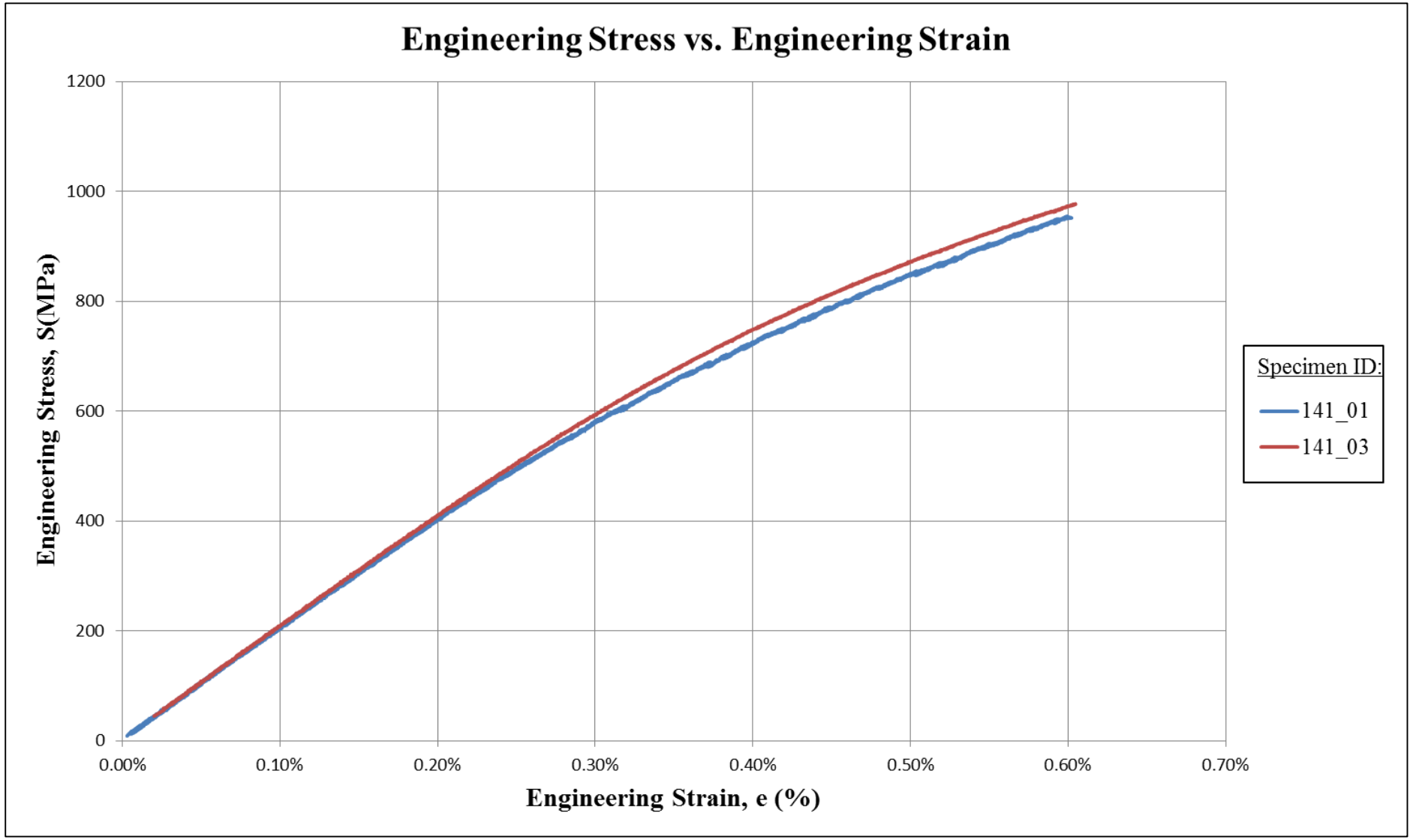

Figure 5: Monotonic stress-strain curves

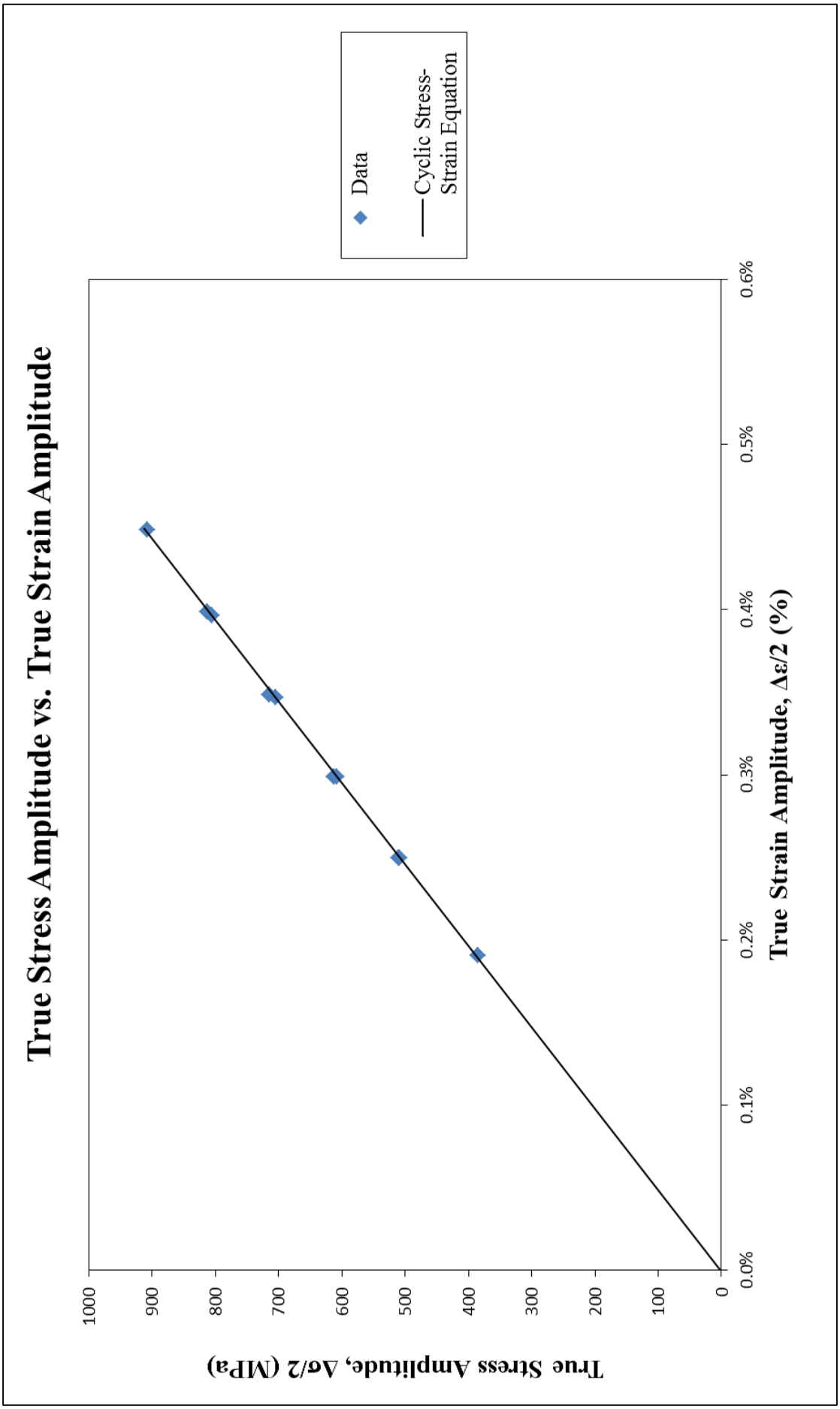

Figure 6: True stress amplitude versus true strain amplitude

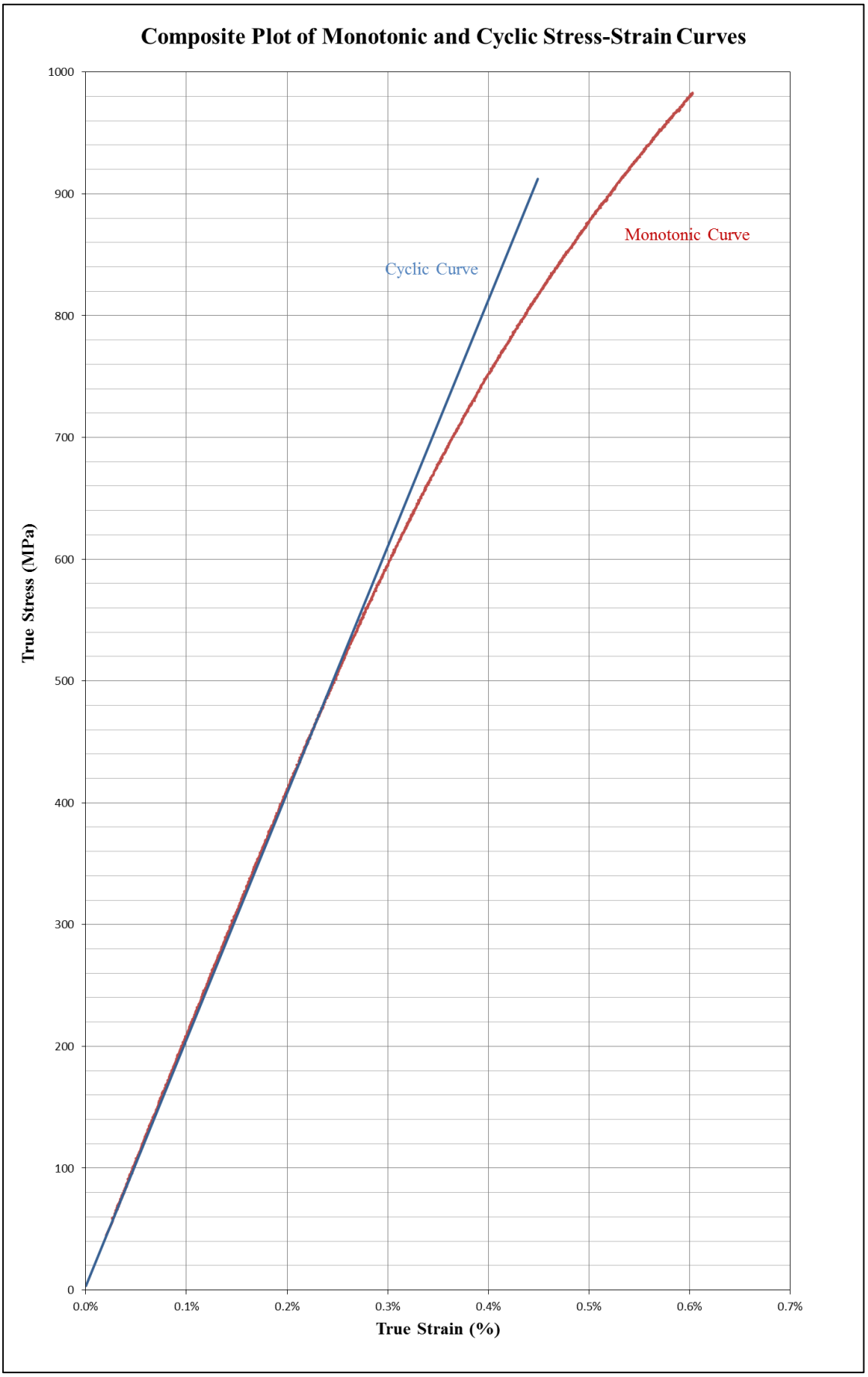

Figure 7: Composite plot of cyclic and monotonic stress-strain curves

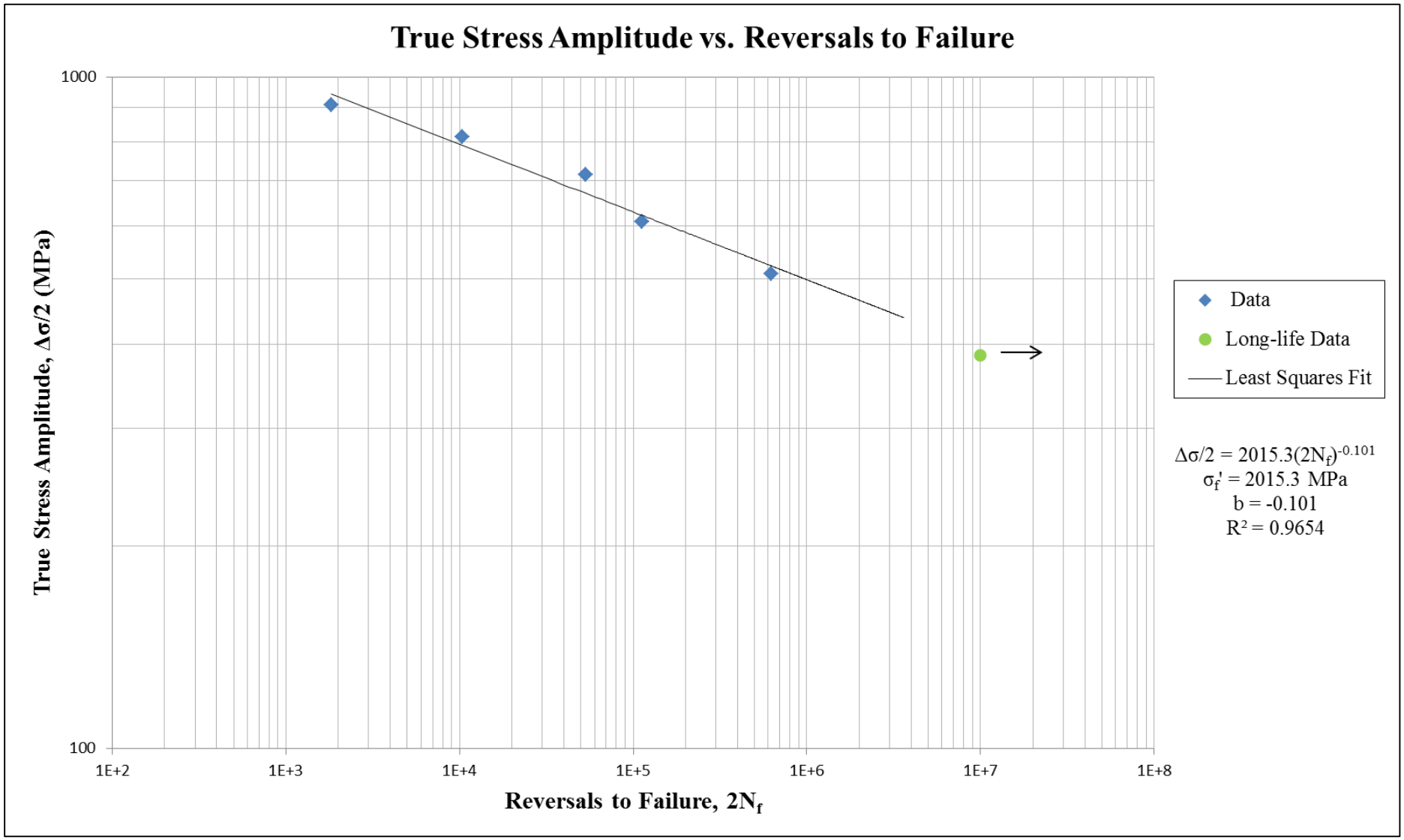

Figure 8: True stress amplitude versus reversals to failure

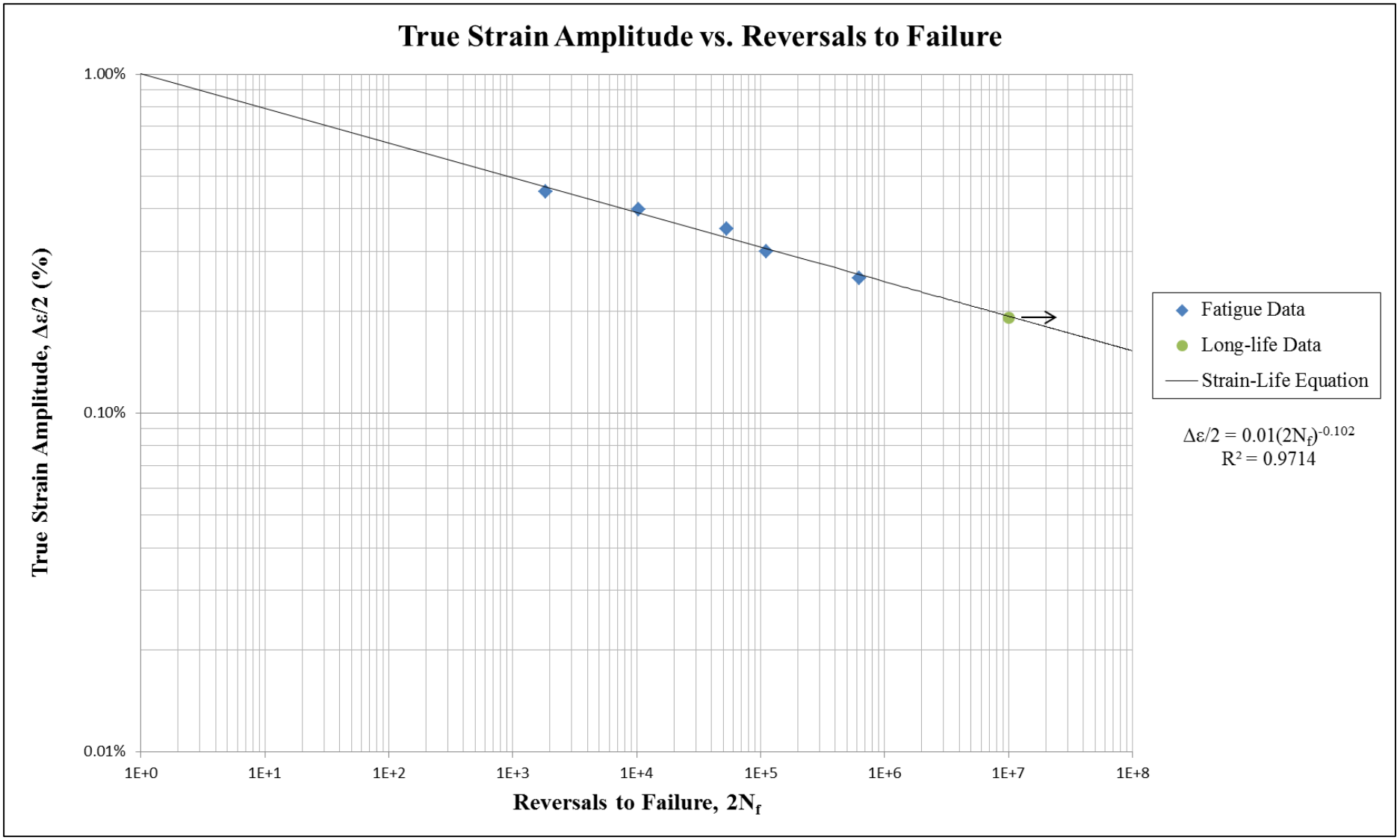

Figure 9: True strain amplitude versus reversals to failure

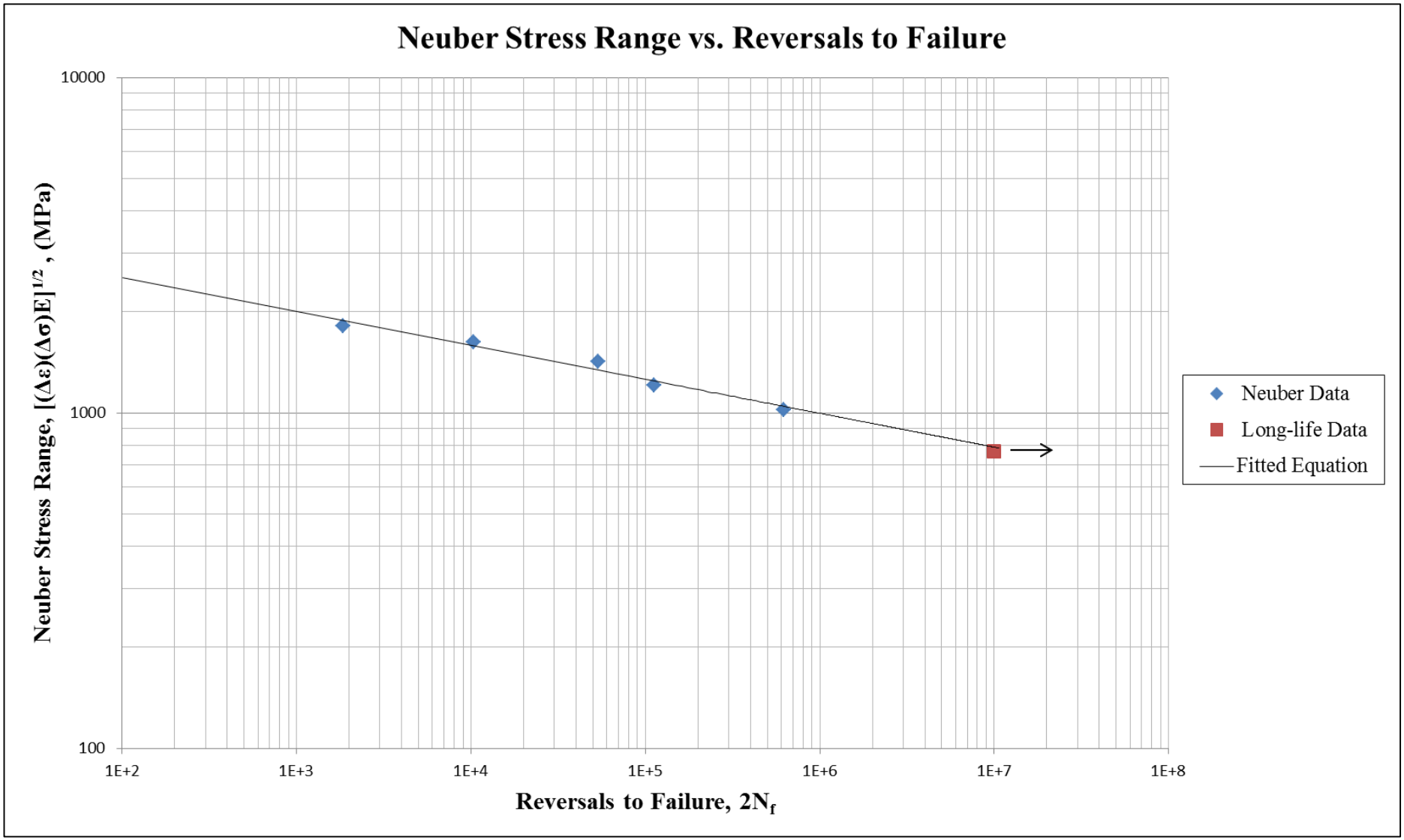

Figure 10: Neuber stress range versus reversals to failure

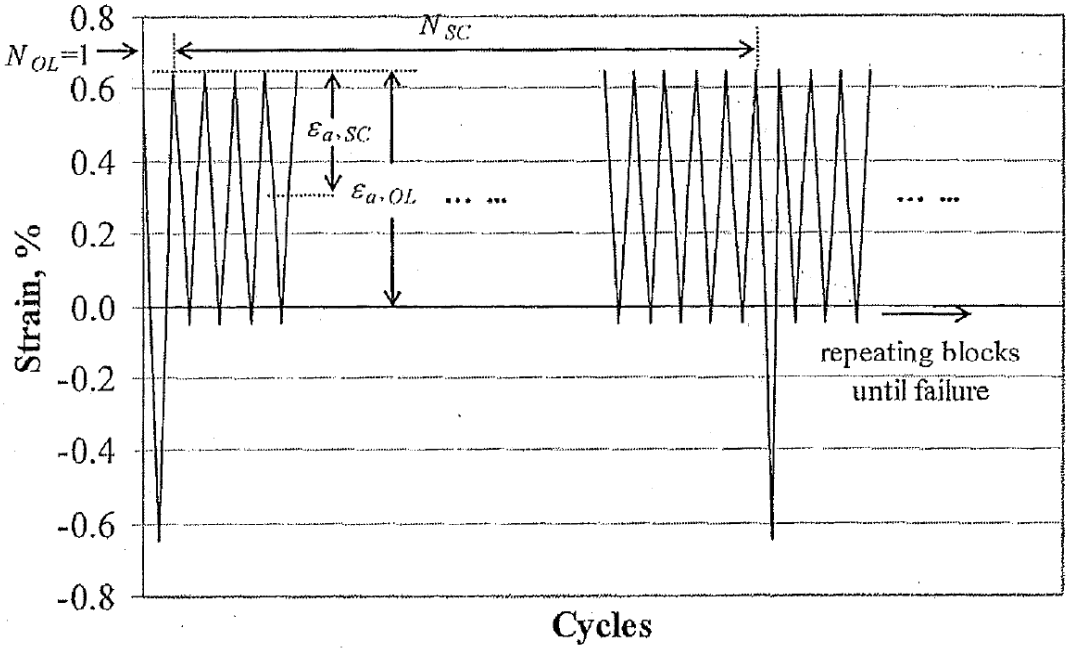

Figure 11: Periodic overload history

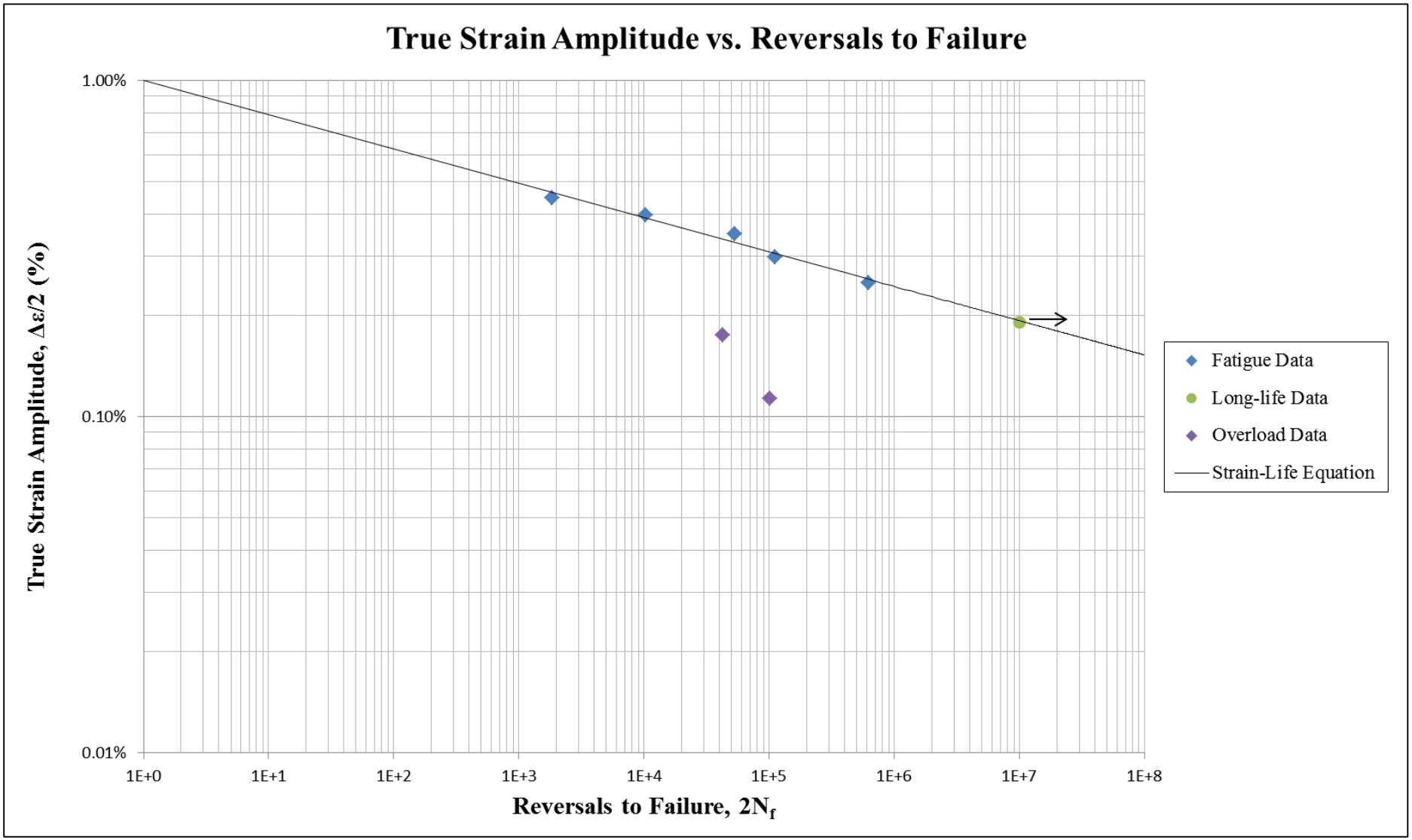

Figure 12: Periodic overload data superimposed with constant amplitude fatigue data

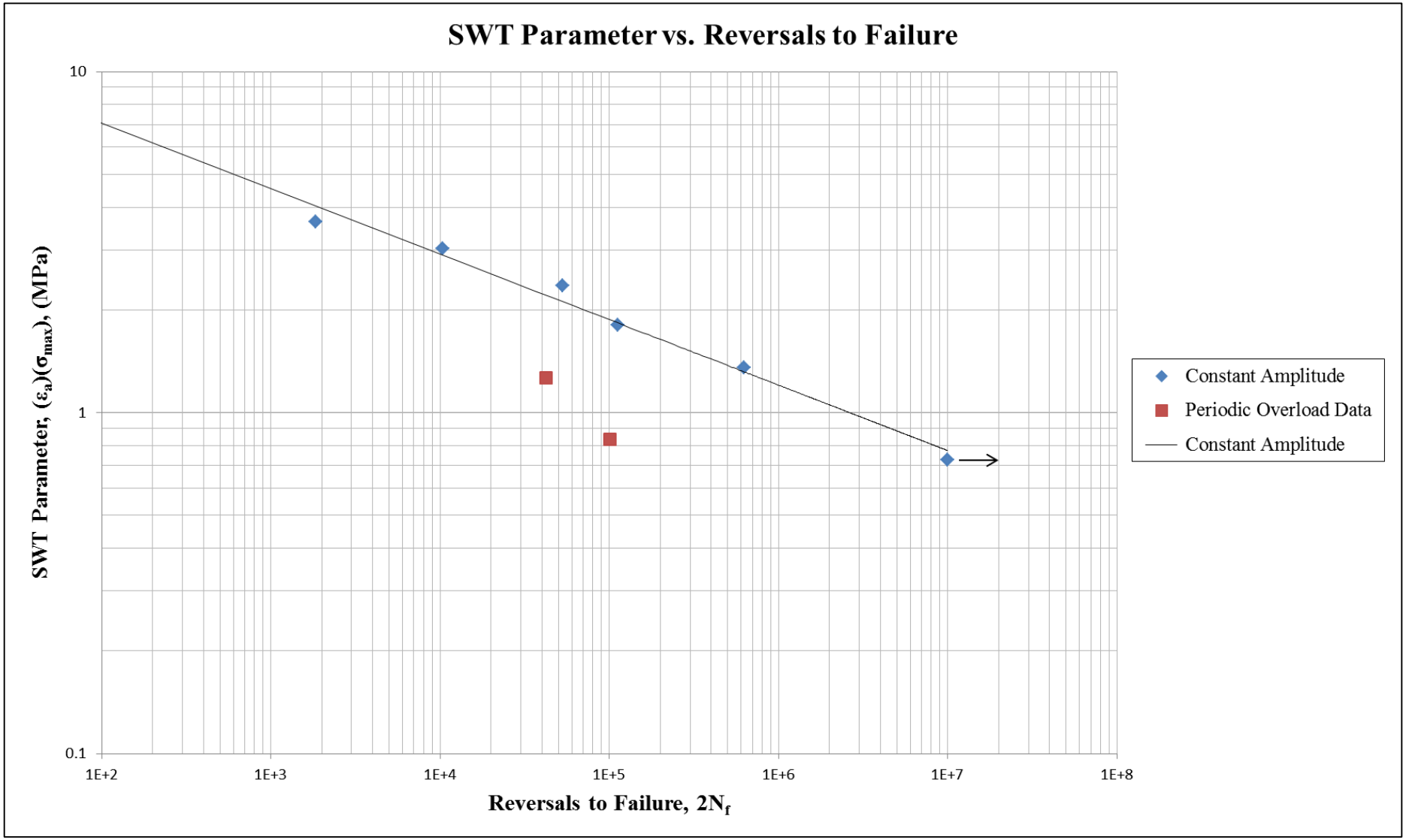

Figure 13: SWT parameter versus reversals to failure. Periodic overload data superimposed on constant amplitude data

REFERENCES

[1] ASTM Standard E606-92, “Standard Practice for Strain-Controlled Fatigue Testing”, Annual Book of ASTM Standards, Vol. 03.01, 2004, pp. 593-606.

[2] ASTM Standard E83-02, “Standard Practice for Verification and Classification of Extensometers”, Annual Book of ASTM Standards, Vol. 03.01, 2004, pp. 232-244.

[3] ASTM Standard E1012-99, “Standard Practice for Verification of Specimen Alignment Under Tensile Loading”, Annual Book of ASTM Standards, Vol. 03.01, 2004, pp. 763-770.

[4] ASTM Standard E8-04, “Standard Test Methods for Tension Testing of Metallic Materials”, Annual Book of ASTM Standards, Vol. 03.01, 2004, pp. 62-85.

[5] ASTM Standard E739-91, “Standard Practice for Statistical Analysis of Linear or Linearized Stress-Life (S-N) and Strain-Life (ε-N) Fatigue data”, Annual Book of ASTM Standards, Vol. 03.01, 1995, pp. 670-676.

[6] ASTM Standard E646-00, “Standard Test Method for Tensile Strain-Hardening Exponents (n-values) of Metallic Sheet Materials”, Annual Book of ASTM Standards, Vol. 03.01, 2004, pp. 619-626.

[7] Stephens R. I., Fatemi A., Stephens R.R. and Fuchs H. O., “*Metal Fatigue in Engineering*”, Second edition, Wiley Interscience, 2000.

[8] Yung-Li Lee, Jwo Pan, Richard Hathaway, Mark Barkey, 2005, “*Fatigue Testing and Analysis*”, Elsevier Inc.

APPENDIX A

Table A.1a: Summary of monotonic tensile test results (Runout in center ≤ 0.006 inches)

Specimen ID	D_0, mm	D_f, mm	L_0, mm	L_f, mm	R, mm	E, GPa	YS, MPa	S_u, MPa	K, MPa	n	%EL	%RA	ε_f %	σ_f MPa
141_01	5.140	5.140	1.207	7.62	7.849	201.1	-	952.4	4336.1	0.2264	3.00%	0%	0	676.7
141_03	5.180	5.180	1.207	7.62	7.892	204.3	-	977.1	3660.1	0.1967	3.57%	0%	0	693.7
AVG.	5.160	5.160	1.207	7.62	7.870	202.7	-	964.8	3998.1	0.2116	3.28%	0%	0	685.2

Table A.1b: Summary of monotonic tensile test results (Runout in center > 0.006 inches)

Specimen ID	D_0, mm	D_f, mm	L_0, mm	L_f, mm	R, mm	E, GPa	YS, MPa	S_u, MPa	K, MPa	n	%EL	%RA	ε_f %	σ_f MPa
141_02	5.110	5.110	1.207	7.62	7.786	204.12	-	679.43	-	-	2.18%	0%	0	483.61

Table A.2a: Summary of constant amplitude completely reversed fatigue test results (Runout in center ≤ 0.006 inches)

Specimen ID	Applied Strain %	Test control mode	Test freq., Hz	E, GPa [e]	At midlife ($N_{50\%}$)							$(2N_f)_{10\%}$, [b] reversals	$(2N_f)_{50\%}$, [c] reversals	Failure location [d]
					E′, GPa	$\Delta\varepsilon/2$, %	$\Delta\varepsilon_p/2$, (calculated) %	$\Delta\varepsilon_p/2$, (measured) %	$\Delta\sigma/2$, MPa	σ_m, MPa	$2N_{50\%}$, [a] reversals			
141_21	±0.45%	strain	0.5	202.0	200.1	0.449%	0.000%	0.000%	907.5	-8.4	918	-	1,836	IGL
141_09	±0.4%	strain	0.8	203.8	200.9	0.399%	0.000%	0.000%	812.8	-2.6	5,168	-	10,334	IGL
141_12	±0.35%	strain	0.8	202.5	202.1	0.349%	0.000%	0.000%	714.0	-6.8	26,622	-	53,242	IGL
141_14	±0.3%	strain load	1.0 5.0	201.1	201.0	0.299%	0.000%	0.000%	608.7	-4.9	55,956	-	111,912	IGL
141_16	±0.25%	strain load	1.0 10.0	205.1	203.3	0.250%	0.000%	0.000%	508.7	3.4	311,254	-	622,508	IGL

Table A.2b: Summary of constant amplitude completely reversed fatigue test results (Runout in center > 0.006 inches)

Specimen ID	Applied Strain %	Test control mode	Test freq., Hz	E, GPa [e]	At midlife ($N_{50\%}$)							$(2N_f)_{10\%}$, [b] reversals	$(2N_f)_{50\%}$, [c] reversals	Failure location [d]
					E′, GPa	$\Delta\varepsilon/2$, %	$\Delta\varepsilon_p/2$, (calculated) %	$\Delta\varepsilon_p/2$, (measured) %	$\Delta\sigma/2$, MPa	σ_m, MPa	$2N_{50\%}$, [a] reversals			
141_08	±0.5%	strain	0.3	205.9	-	0.500%	-	-	-	-	-	-	1	IGL
141_10	±0.4%	strain	0.8	200.4	200.3	0.397%	0.000%	0.000%	805.1	-10.1	536	-	1,072	IGL
141_11	±0.35%	strain	0.8	198.3	200.0	0.347%	0.000%	0.000%	704.9	-3.6	574	-	1,146	IGL
141_13	±0.3%	strain load	1.0 5.0	202.5	201.7	0.299%	0.000%	0.000%	612.6	-8.1	24,682	-	49,364	IGL
141_15	±0.25%	strain load	1.0 10.0	202.1	203.4	0.250%	0.000%	0.000%	510.7	-4.3	88,968	-	177,934	IGL
141_17	±0.2%	strain load	1.0 20.0	200.4	200.4	0.191%	0.000%	0.000%	385.0	-5.0	500,000	-	>10,000,000	No Failure

[a] $2N_{50\%}$ is defined as the midlife reversal;

[b] $(2N_f)_{10\%}$ is defined as reversal of 10% load drop;

[c] $(2N_f)_{50\%}$ is defined as reversal of 50% load drop or failure;

[d] IGL = Inside gage length

[e] E value was calculated from the first cycle.

Table A.3: Measurement of Specimen Dimensions

Specimen ID	Total Length (mm)	Grip Diameter* (mm)	Grip Length* (mm)	Gage Diameter (mm)	Gage Length (mm)
141_01	110.63	12.68	38.70/40.01	5.14	7.62
141_02	111.74	12.67	39.27/40.86	5.11	7.62
141_03	111.46	12.71	38.96/39.81	5.18	7.62
141_04	111.50	12.70	39.50/40.50	5.25	7.62
141_05	109.94	12.73	38.71/39.30	5.16	7.62
141_08	112.60	12.75	39.25/41.65	5.19	7.62
141_09	111.12	12.72	38.73/40.83	5.17	7.62
141_10	110.38	12.72/12.75	39.02/39.51	5.19	7.62
141_11	110.42	12.72	39.04/40.09	5.13	7.62
141_12	110.18	12.72	38.60/39.72	5.12	7.62
141_13	112.83	12.65	38.92/42.02	5.16	7.62
141_14	110.15	12.73	39.04/39.40	5.18	7.62
141_15	110.86	12.64	39.18/40.46	5.21	7.62
141_16	111.37	12.70	38.92	5.12	7.62
141_17	110.76	12.54	38.60/40.55	5.13	7.62
141_21	111.69	12.66	38.19/41.42	5.15	7.62
142_01	111.44	12.65/12.70	39.19/40.00	5.21	7.62
142_02	111.54	12.70/12.78	38.96/41.3	5.18	7.62
142_03	110.61	12.70	39.03/39.94	5.17	7.62
142_04	110.90	12.76	38.85/40.17	5.12	7.62
142_05	109.22	12.76	38.69/38.85	5.13	7.62
142_06	107.70	12.72/12.68	39.03	5.13	7.62

* For some of the specimens, the grip length and the grip diameter of one side is different from the other side. Both dimensions are provided in the table.

Table A.4: AISI Test Bars (20MoCr4 Carburized Case)

	RUNOUT IN CENTER (INCH)		
Specimen ID	Before HT	After HT	Change
141_01	0.0018	0.0115 ×	0.0097
141_02	0.0019	0.0314 ×	0.0295
141_03	0.0016	0.0152 ×	0.0135
141_04	0.0014	0.0040	0.0026
141_05	0.0023	0.0049	0.0026
141_08	0.0017	0.0174 ×	0.0157
141_09	0.0024	0.0043	0.0019
141_10	0.0016	0.0200 ×	0.0183
141_11		0.0194 ×	
141_12		0.0052	
141_13		0.0112 ×	
141_14		0.0041	
141_15		0.0063 ×	
141_16		0.0025	
141_17		0.0126 ×	
141_21		0.0051	
141_22		0.0152 ×	
141_23		0.0316 ×	
141_24		0.0128 ×	
142_01	0.0009	0.0029	0.0020
142_02	0.0009	0.0020	0.0011
142_03		0.0177 ×	
142_04		0.0082 ×	
142_05		0.0078 ×	
142_06		0.0159 ×	

Note: "×" means the runout in center of specimen exceeds the 0.006-inch limit after the heat treatment, which may affect the test results.

Table A.5a: Summary of periodic overload fatigue test results (Runout in center ≤ 0.006 inches)

Spec. ID	Test Control mode	Test Freq. OL/SC (Hz)	E (GPa) [a]	Load History Description											Exp.Life (Blks)	$N_{f,SC(eq)}$ (Cycles)	OL Damage Ratio	Failure Location [b]
				$\varepsilon_{a,SC}$ (%)	$\varepsilon_{m,SC}$ (%)	$\Delta\varepsilon_p/2,SC$ (calculated) (%)	$\sigma_{a,SC}$ (MPa)	$\sigma_{m,SC}$ (MPa)	N_{SC} (Cycles)	$\varepsilon_{a,OL}$ (%)	$\Delta\varepsilon_p/2,OL$ (calculated) (%)	$\sigma_{a,OL}$ (MPa)	$\sigma_{m,OL}$ (MPa)	$N_{f,OL}$ (Cycles)				
142_01	Strain	1/4	200.3	0.175%	0.164%	0.000%	354.3	366.9	500	0.364%	0.000%	736.5	-12.5	10,000	42	21088	0.0042	IGL
142_02	Strain	1/4	202.4	0.113%	0.289%	0.000%	227.5	512.0	500	0.364%	0.000%	736.2	3.0	10,000	100	50505	0.0100	IGL

Table A.5b: Summary of periodic overload fatigue test results (Runout in center > 0.006 inches)

Spec. ID	Test Control mode	Test Freq. OL/SC (Hz)	E (GPa) [a]	Load History Description											Exp.Life (Blks)	$N_{f,SC(eq)}$ (Cycles)	OL Damage Ratio	Failure Location [b]
				$\varepsilon_{a,SC}$ (%)	$\varepsilon_{m,SC}$ (%)	$\Delta\varepsilon_p/2,SC$ (calculated) (%)	$\sigma_{a,SC}$ (MPa)	$\sigma_{m,SC}$ (MPa)	N_{SC} (Cycles)	$\varepsilon_{a,OL}$ (%)	$\Delta\varepsilon_p/2,OL$ (calculated) (%)	$\sigma_{a,OL}$ (MPa)	$\sigma_{m,OL}$ (MPa)	$N_{f,OL}$ (Cycles)				
142_03	Strain	1/4	200.4	0.175%	0.289%	0.000%	353.8	341.8	100	0.364%	0.000%	733.8	-37.8	10,000	156	15847	0.0156	IGL
142_04	Strain	1/7	205.8	0.111%	0.164%	0.000%	226.1	513.3	1000	0.364%	0.000%	734.7	3.2	10,000	22	22048	0.0022	IGL
142_05	Strain	1/4	204.2	0.200%	-0.06%	0.000%	408.7	248.7	100	0.340%	0.000%	694.0	-36.4	10,000	681	73076	0.0681	IGL
142_06	Strain	1/7	200.6	0.105%	0.095%	0.000%	211.3	381.2	1000	0.305%	0.000%	624.8	-31.9	10,000	69	69479	0.0069	IGL

[a] E value was calculated from the first cycle;

[b] IGL = Inside gage length, KE = At knife edge.

All stress values reported are from midlife.

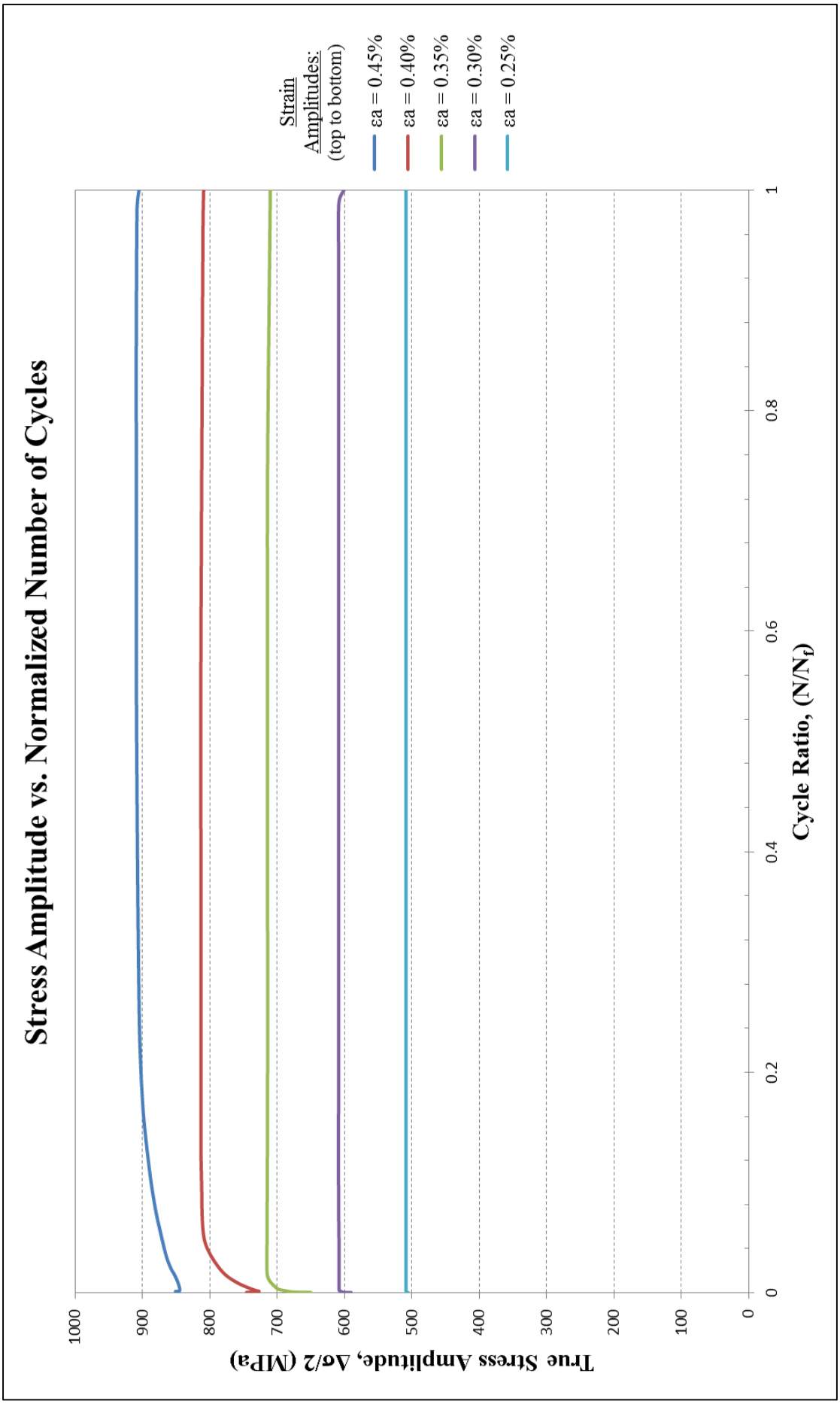

Figure A.1a: True stress amplitude versus normalized number of cycles

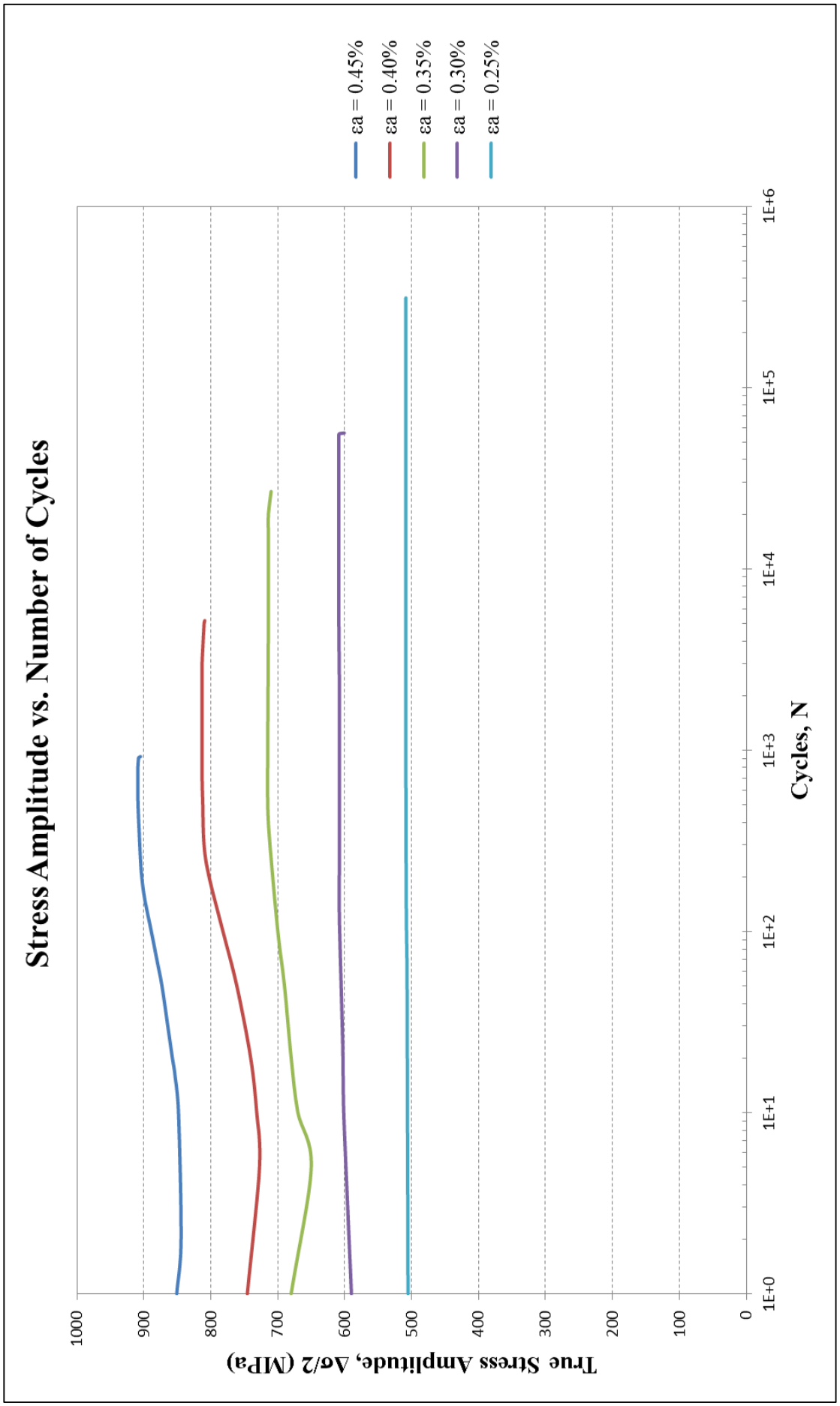

Figure A.1b: True stress amplitude versus number of cycles

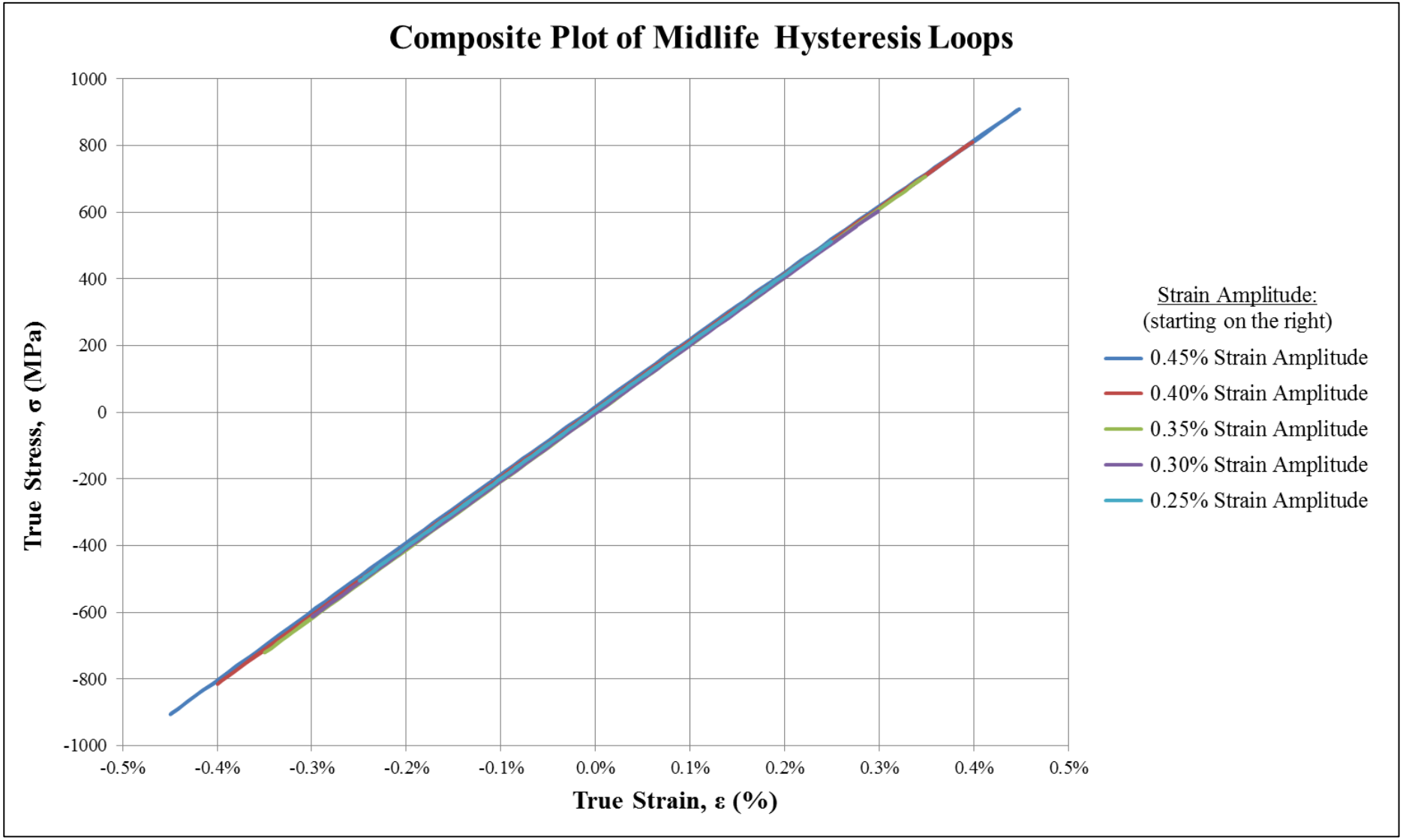

Figure A.2: Composite plot of midlife hysteresis loops

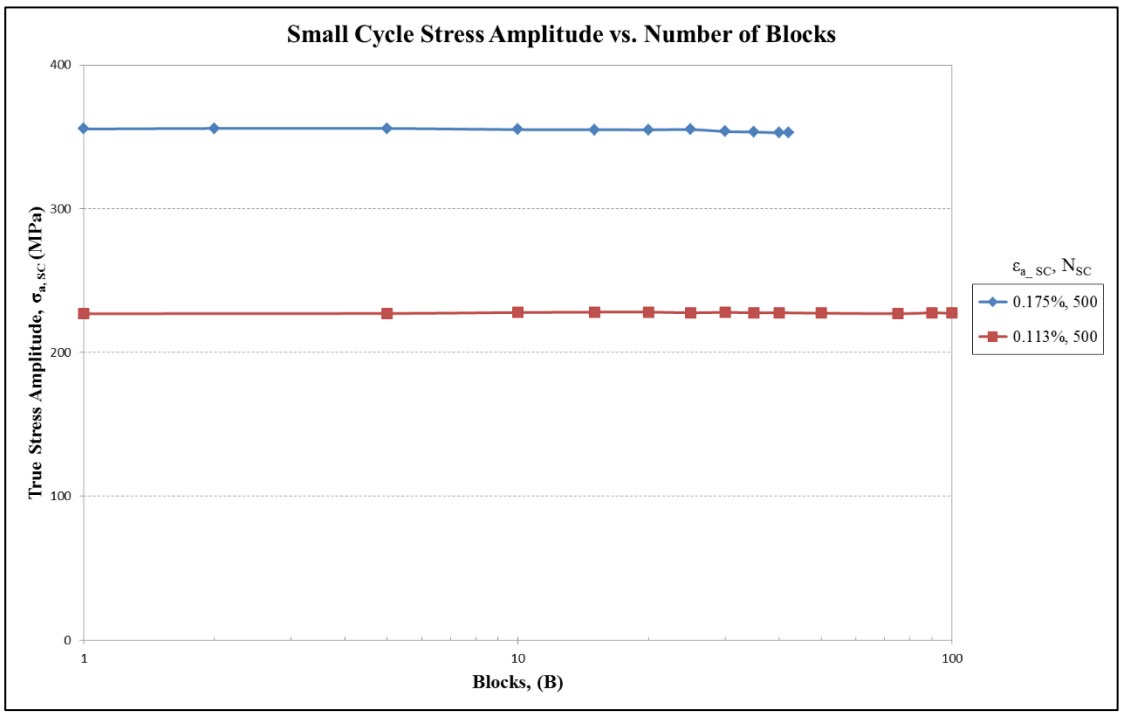

Figure A.3a: Small cycle amplitude transient response throughout the life

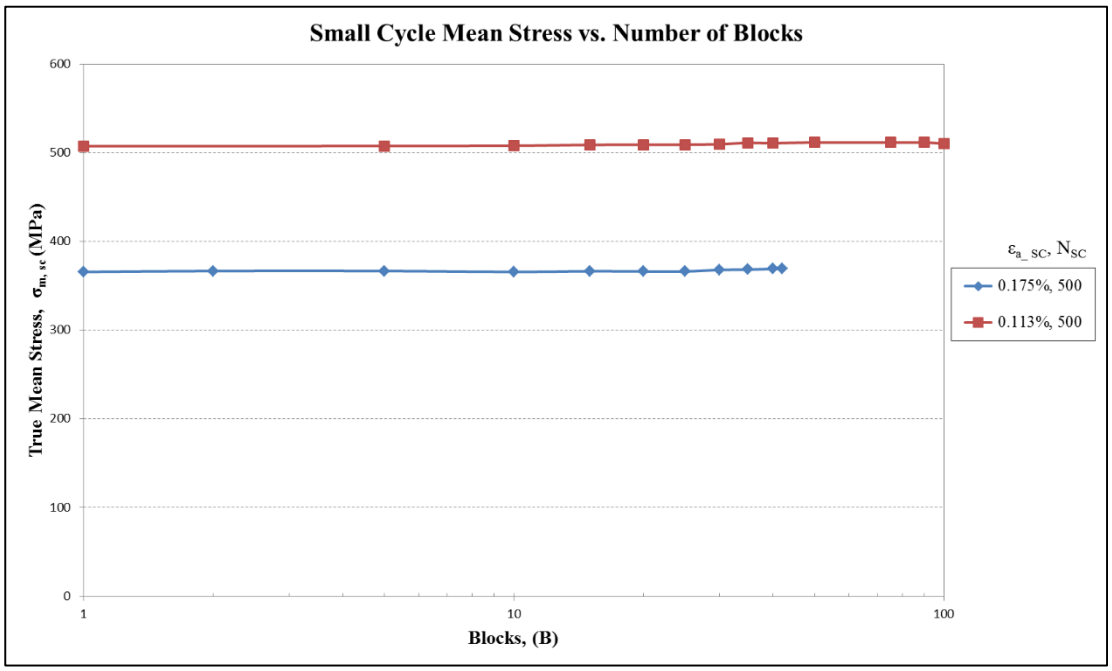

Figure A.3b: Small cycle mean transient response throughout the life

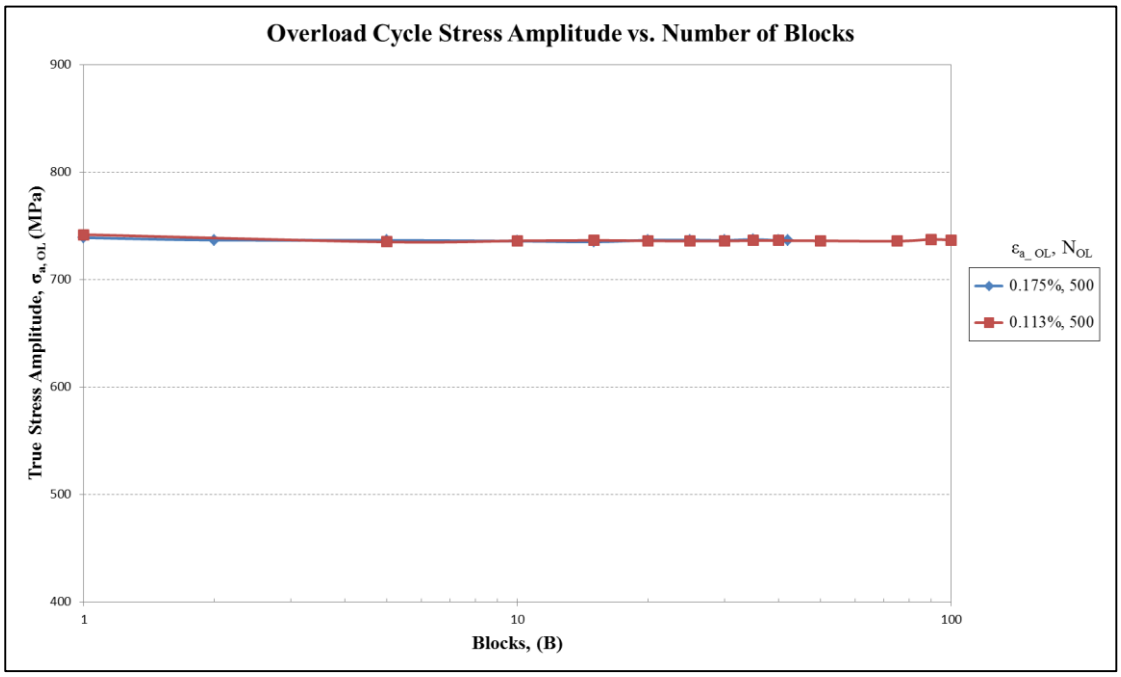

Figure A.4a: Overload cycle amplitude transient response throughout the life

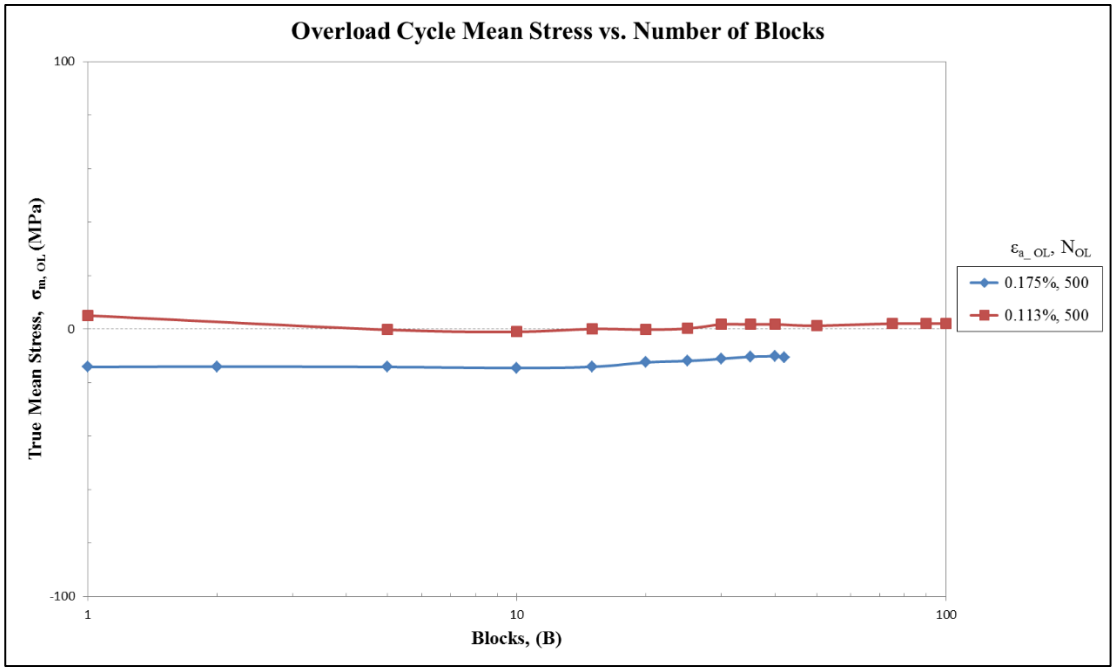

Figure A.4b: Overload cycle mean transient response throughout the life

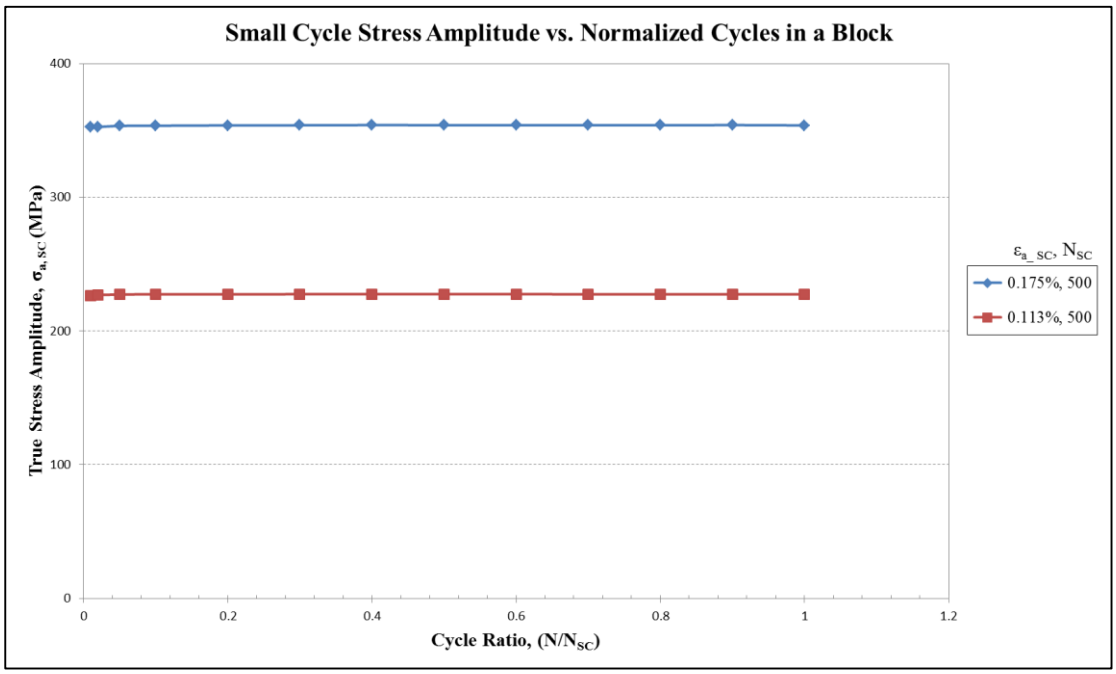

Figure A.5a: Small cycle transient response amplitude throughout one load block at midlife

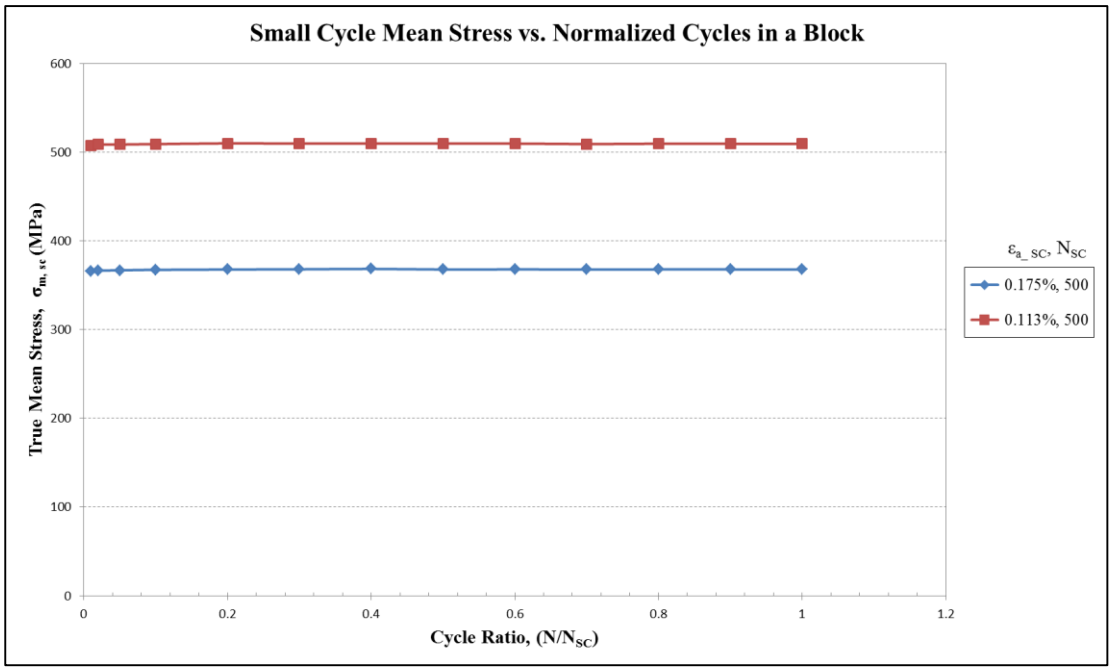

Figure A.5b: Small cycle transient response mean throughout one load block at midlife

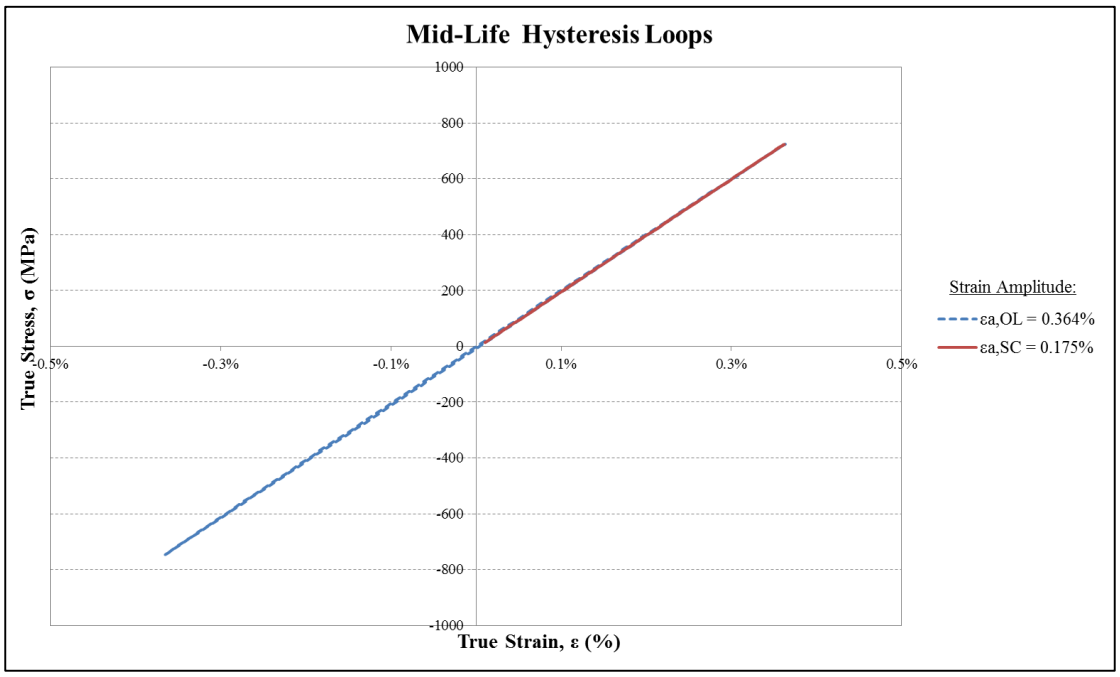

(a)

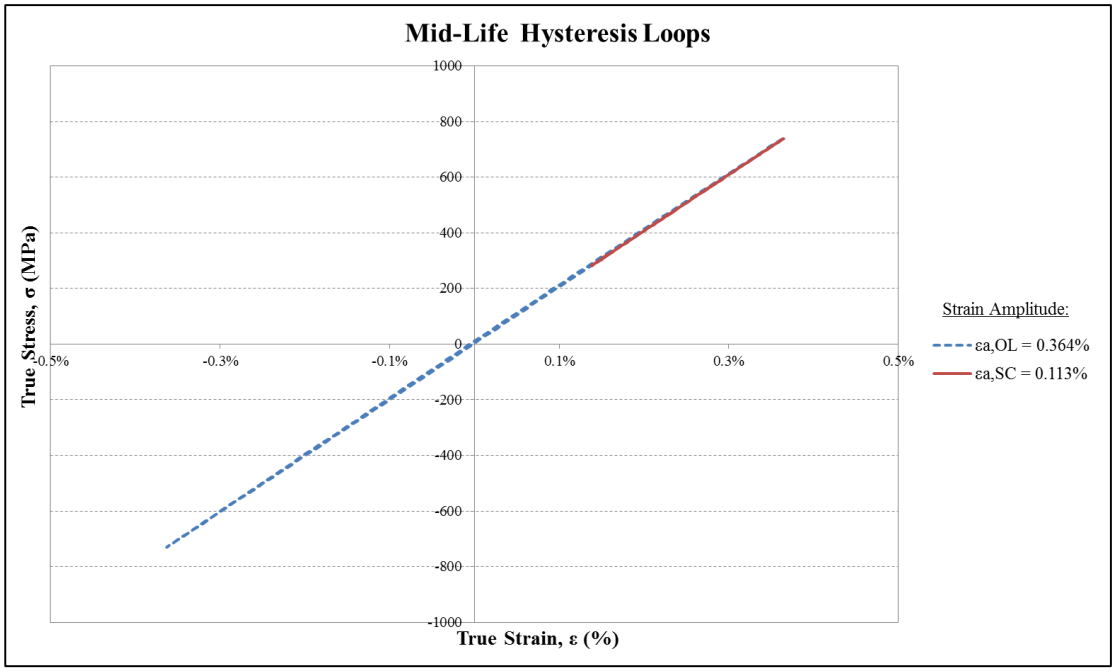

(b)

Figure A.6(a-b): Periodic overload midlife hysterisis loop superimposed with small cycle midlife hysterisis loop

APPENDIX B

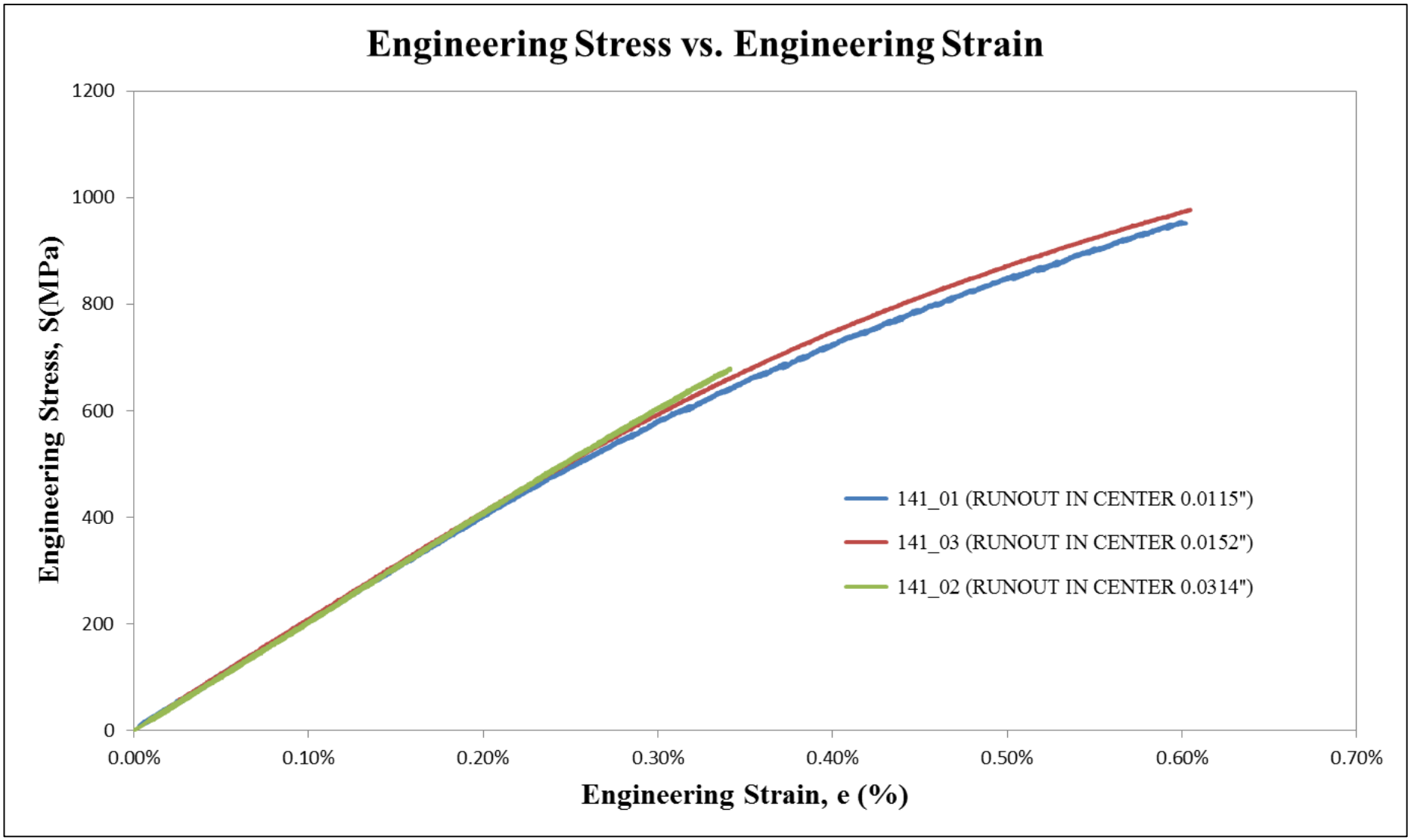

Figure B.1: Monotonic stress-strain curves (Comparison between big runout and small runout specimens)

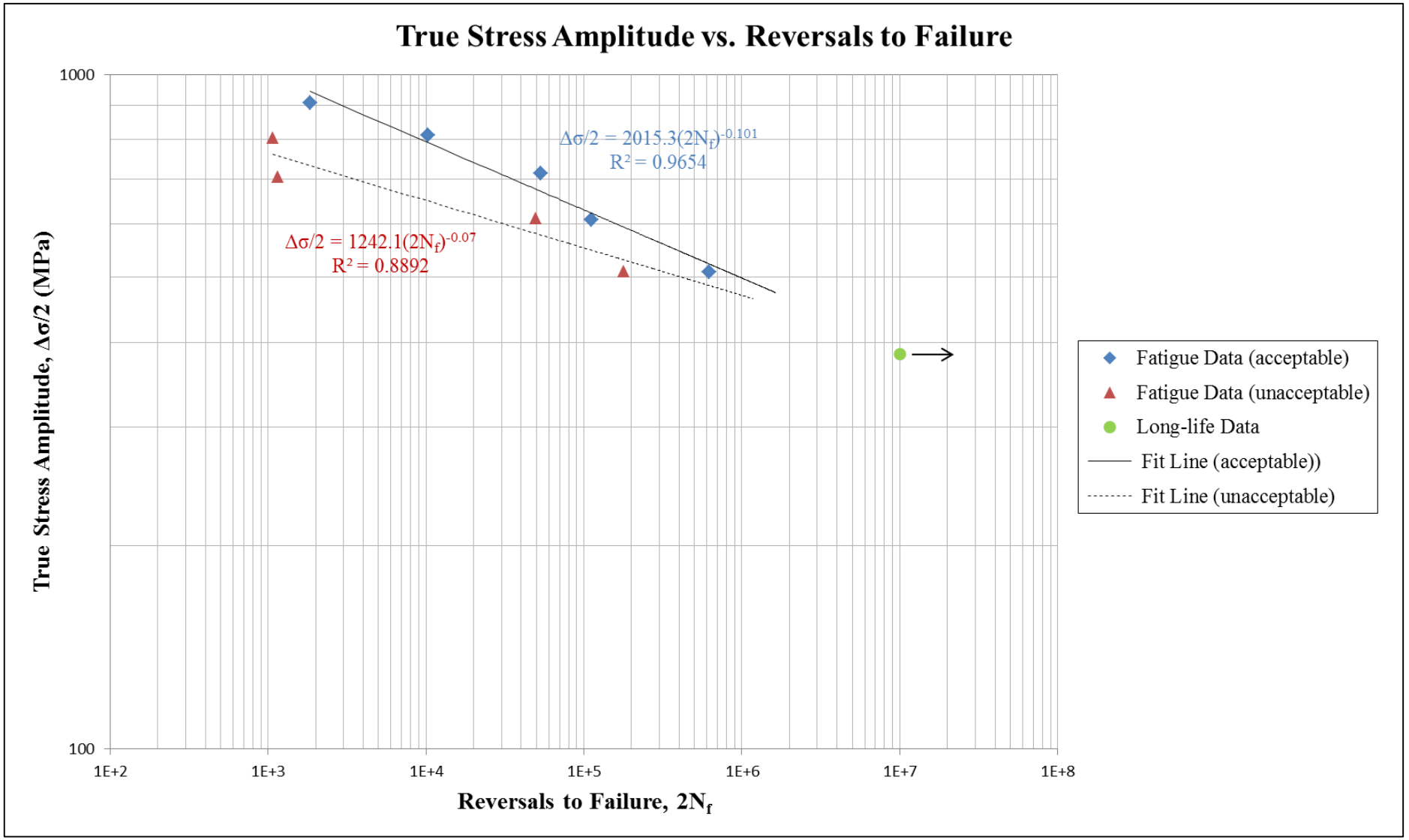

Figure B.2: True stress amplitude versus reversals to failure (Comparison between big runout and small runout specimens)

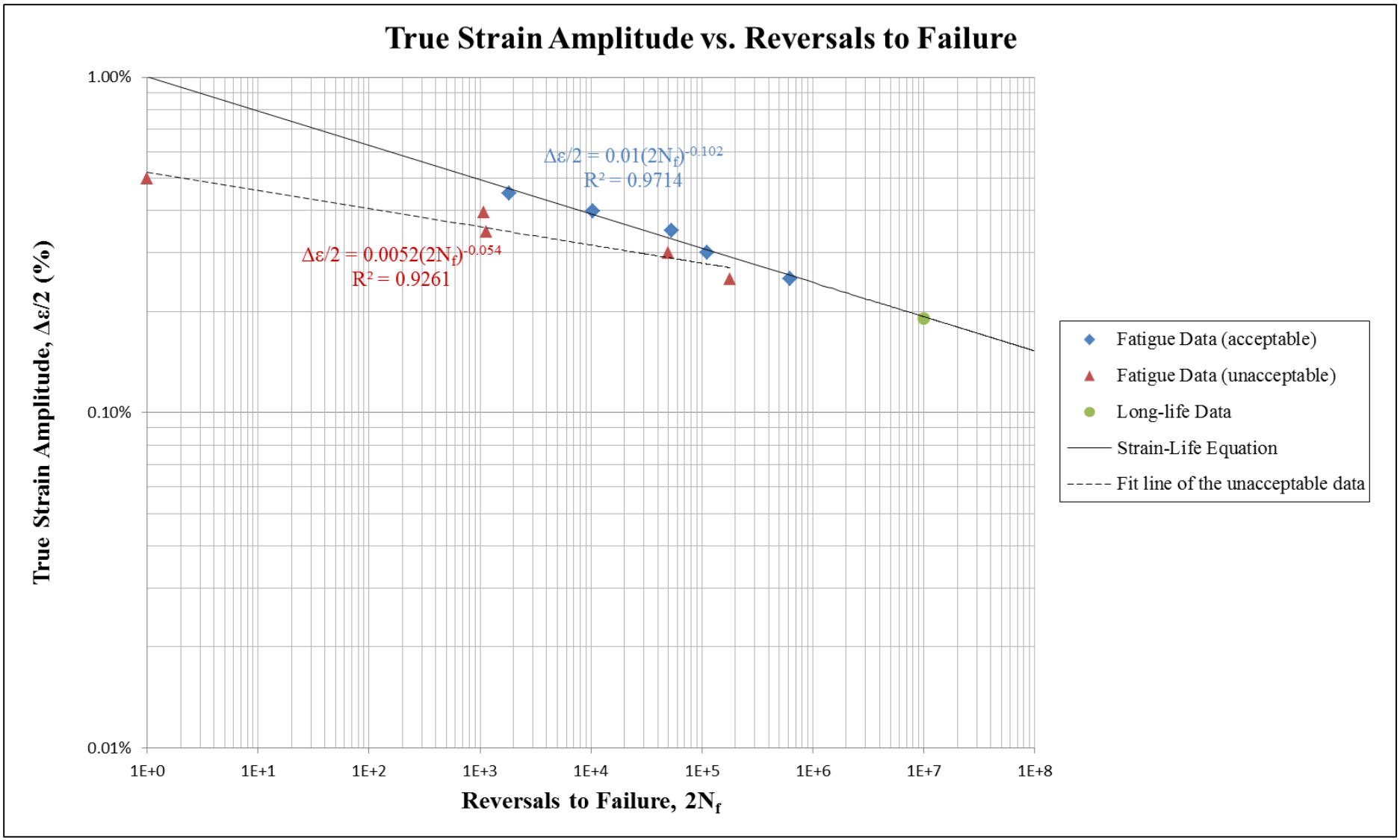

Figure B.3: True strain amplitude versus reversals to failure (Comparison between big runout and small runout specimens)

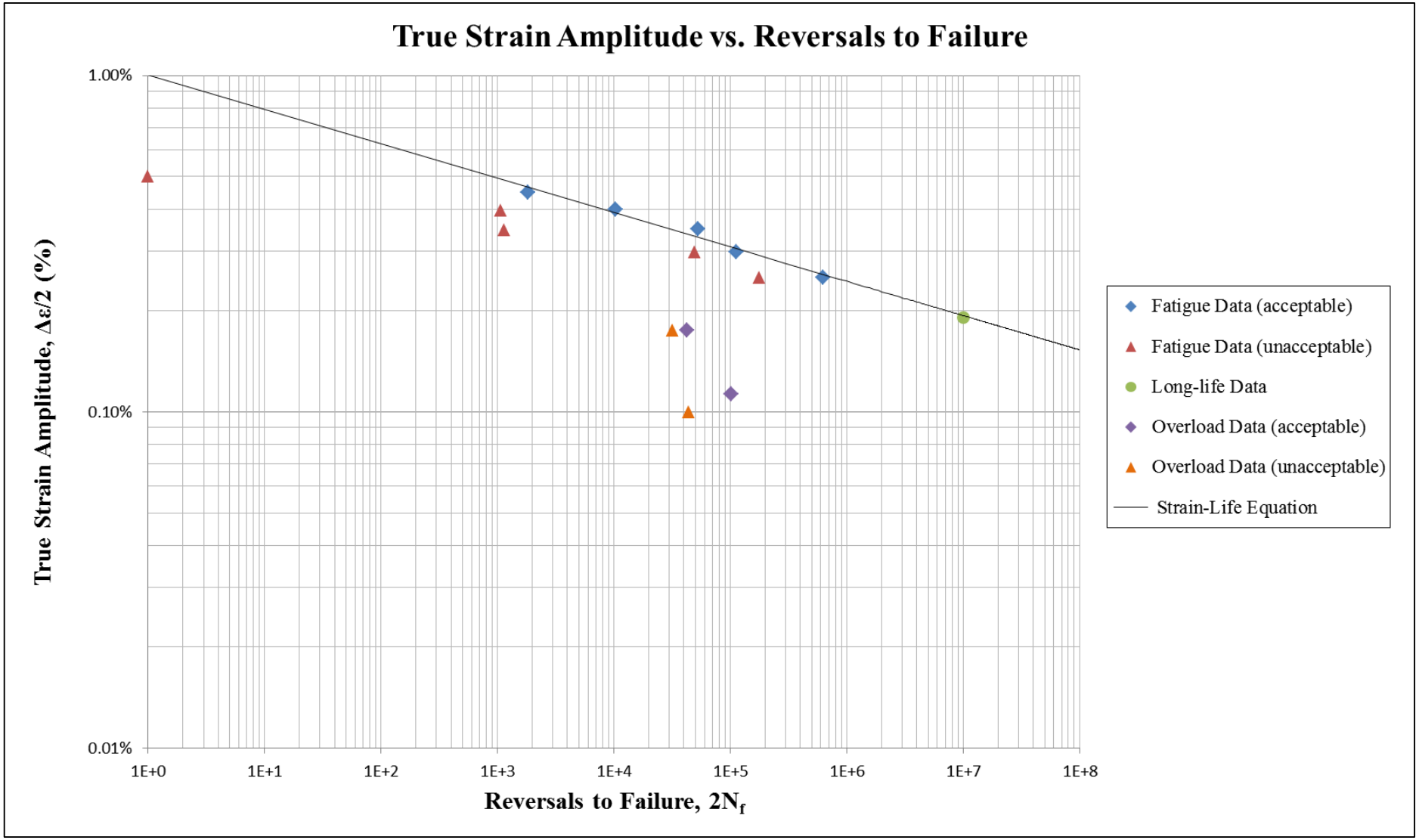

Figure B.4: Periodic overload data superimposed with constant amplitude fatigue data (Comparison between big runout and small runout specimens)